Linear Oligo(ferrocenyldimethylsilanes) with between Two and Nine Ferrocene Units: Electrochemical and Structural Models for Poly(ferrocenylsilane) High Polymers

Ron Rulkens,[†] Alan J. Lough,[†] Ian Manners,*[,†] Sherri R. Lovelace,[‡] Casey Grant,[‡] and William E. Geiger*[,‡]

Contribution from the Department of Chemistry, University of Toronto, 80 St. George Street, Toronto, Ontario, M5S 3H6, Canada, and the Department of Chemistry, University of Vermont, Burlington, Vermont 05405-0125

Received July 17, 1996[⊗]

Abstract: In order to gain insight into the electrochemical and conformational properties of the prototypical high polymeric poly(ferrocenylsilane), poly(ferrocenyldimethylsilane) $[Fe(\eta\text{-}C_5H_4)_2SiMe_2]_n$ **6**, three series of oligo(ferrocenylsilanes) R-fc-$[SiMe_2\text{-fc}]_{n-1}$-R′ (fc = $Fe(\eta\text{-}C_5H_4)_2$) $\mathbf{7_2}-\mathbf{7_9}$ (R = R′ = H), $\mathbf{8_2}-\mathbf{8_7}$ (R = H and R′ = $SiMe_3$), and $\mathbf{9_2}-\mathbf{9_7}$ (R = R′ = $SiMe_3$) have been prepared and studied (the subscript n in the oligomer refers to the number of ferrocene units present). These species were prepared via the anionic ring-opening oligomerization of the silicon-bridged [1]ferrocenophane $Fe(\eta\text{-}C_5H_4)_2SiMe_2$ **5**. Initiation with ferrocenyllithium FcLi (Fc = $Fe(\eta\text{-}C_5H_5)(\eta\text{-}C_5H_4)$) followed by quenching with H_2O or $SiMe_3Cl$ afforded H-fc-$[SiMe_2\text{-fc}]_{n-1}$-H ($\mathbf{7_{2-9}}$) or H-fc-$[SiMe_2\text{-fc}]_{n-1}$-$SiMe_3$ ($\mathbf{8_{2-7}}$), respectively. Initiation with the dilithioferrocene complex fcLi·$^2/_3$TMEDA followed by quenching with H_2O or $SiMe_3Cl$ similarly afforded the oligomers H-fc-$[SiMe_2\text{-fc}]_{n-1}$-H ($\mathbf{7_{2-9}}$) or alternatively the bis(silyl)-capped species Me_3Si-fc-$[SiMe_2\text{-fc}]_{n-1}$-$SiMe_3$ ($\mathbf{9_{2-7}}$), respectively. The individual molecular compounds of these three series of oligomers $\mathbf{7_2}-\mathbf{7_9}$, $\mathbf{8_2}-\mathbf{8_7}$, and $\mathbf{9_2}-\mathbf{9_7}$ were isolated in pure form from the oligomeric mixtures by column chromatography and these were structurally characterized by ^1H, ^{13}C, and ^{29}Si NMR spectroscopy, mass spectrometry, and in selected cases by elemental analysis. The structure of the linear pentamer $\mathbf{7_5}$ has also been determined by single crystal X-ray diffraction. The central portion of this species possesses a trans planar zigzag conformation in the solid state and appears to be a valuable model for the analogous conformation of the high polymer **6** in crystalline domains. The electrochemical behavior of each pure oligomer was studied by cyclic and differential pulse voltammetry and was found to depend on whether an odd or an even number of ferrocene units were present. For oligomer systems containing an odd number of iron centers two reversible redox processes of varying intensities at −0.02−0.00 V and 0.21−0.23 V (vs ferrocene) were observed with a redox splitting of 0.21−0.23 V. For oligomer systems containing an even number of iron centers larger then two, three reversible redox processes of varying intensities were observed at ca. 0.00, 0.13, and 0.24 V vs ferrocene. As the oligomer chain length increased, the electrochemical behavior for both the "odd" and "even" series approached that of the high polymer **6** for which two reversible redox processes at 0.00 and 0.24 V (vs ferrocene) of equal intensity exist. These results are completely consistent with the previously proposed theory that initial oxidation of **6** affords a product in which alternating iron sites are oxidized. Spectroelectrochemical experiments show an intervalence electron transfer absorption (1100−1350 nm, $\epsilon_{max} \leqslant 150$ M^{-1} cm^{-1}) for partially oxidized oligo(ferrocenylsilanes) that is typical for class II mixed-valent compounds. Additionally, single crystals were obtained of the mixed-valent linear trimer, $\mathbf{7_3}^{2+}$, as an I_3^- salt and a single crystal X-ray diffraction study revealed the presence of terminal ferrocenium centers and a central ferrocene group consistent with the alternating iron oxidation concept.

Introduction

Binuclear transition metal complexes in which the metal atoms are in close enough proximity to permit through space or bridging ligand-mediated interactions have been well-studied.[1−4] This is particularly the case for biferrocenes which yield mixed-valent monocations (e.g., **1** and **2**)[5,6] that possess delocalization on a variety of different time scales depending on subtle structural factors and even solid state environmental effects.[7,8] Recently, oligomeric metallocene-based species have attracted attention with respect to their electrochemical, electronic, and magnetic properties.[8−15]

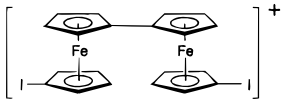

1

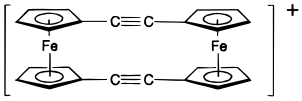

2

High polymers in which the metal atoms interact with one another are also of considerable interest but most well-characterized examples of such materials have been prepared only recently.[16,17] Ferrocene-backbone polymers with high

[†] University of Toronto.
[‡] University of Vermont.
[⊗] Abstract published in *Advance ACS Abstracts,* November 1, 1996.

(1) Geiger, W. E.; Connelly, N. G. *Adv. Organomet. Chem.* **1985**, *24*, 87.
(2) Hush, N. S. *Prog. Inorg. Chem.* **1967**, *8*, 391.
(3) Le Narvor, N.; Toupet, L.; Lapinte, C. *J. Am. Chem. Soc.* **1995**, *117*, 7129.
(4) Tolbert, L. M.; Zhao, X.; Ding, Y.; Bottomley, L. A. *J. Am. Chem. Soc.* **1995**, *117*, 12891.
(5) Kramer, J. A.; Hendrickson, D. N. *Inorg. Chem.* **1980**, *19*, 3330.
(6) Morrison, W. H.; Hendrickson, D. N. *Inorg. Chem.* **1975**, *14*, 2331.
(7) Dong, T.-Y.; Huang, C.-H.; Chang, C.-K.; Hsieh, H.-C.; Peng, S.-M.; Lee, G.-H. *Organometallics* **1995**, *14*, 1776−1785.
(8) Dong, T.-Y.; Lee, S.-H.; Chang, C.-K.; Lin, K.-J. *J. Chem. Soc., Chem. Commun.* **1995**, 2453.

S0002-7863(96)02470-5 CCC: $12.00

Scheme 1. Synthesis of Poly(ferrocenes)

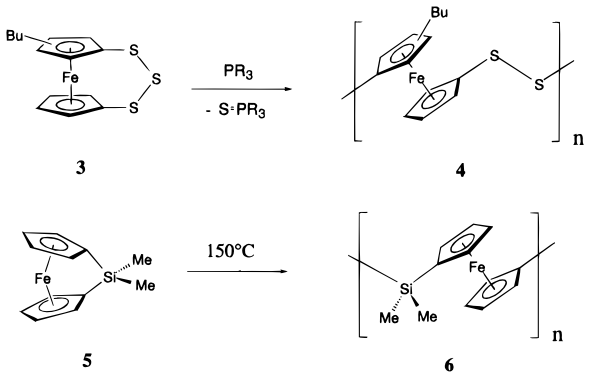

molecular weights (M_n > 10 000) and interacting metal atoms were first reported in 1992 (Scheme 1).[18,19] Initially, the synthesis of poly(ferrocenylene persulfides) **4** from [3]trithiaferrocenophanes **3** by a novel atom-abstraction route was described by Rauchfuss and co-workers.[18] Shortly thereafter, the preparation of high molecular weight poly(ferrocenylsilanes) such as **6** by the thermal ring-opening polymerization of strained, ring-tilted silicon-bridged [1]ferrocenophanes (e.g., **5**) was reported by the Manners group.[19] In each case, electrochemical studies of the polymers by cyclic voltammetry demonstrated the presence of two reversible oxidation waves of equal intensity. It was postulated that due to the interactions between the iron atoms, initial oxidation occurs at alternating iron sites and that subsequent oxidation of the remaining iron(II) centers is energetically less favorable and therefore occurs at a higher potential.[18,19] Subsequent work on analogs of these and related polymers with other spacer groups (e.g., GeR_2, PR) has demonstrated that such materials exhibit similar two-wave electrochemical behavior and a similar explanation in terms of initial oxidation at alternating iron atoms has been invoked.[20−27] It should be noted that, in contrast to poly(ferrocenylenepersulfides) and poly(ferrocenylsilanes) and related materials, ferrocene-based polymers in which the organometallic units are spaced far apart or are in the side group structure show only very weak or non-existent interactions between the iron centers.[28−30] For example, poly(vinylferrocene) shows only a single reversible oxidation wave by cyclic voltammetry.[28]

In order to gain detailed insight into the electrochemical behavior of poly(ferrocenylsilanes) and related polymers and in particular to test the validity of the "alternating iron oxidation" concept, the study of a series of well-defined oligomers would be very desirable. However, in general, the number of reported electrochemical investigations of oligo(ferrocenes) decreases rapidly as the number of metallocene groups increases. To our knowledge, no electrochemical studies have been reported for oligomers which contain more than four metallocene units. Recently, we reported the synthesis of a series of oligo(ferrocenyldimethylsilanes) containing between 2 and 8 ferrocene units via the anionic oligomerization of the silicon-bridged [1]ferrocenophane **5** using ferrocenyllithium as initiator.[31−33] The synthesis of oligo(ferrocenes) by anionic ring-opening oligomerization is essentially different from the normal approaches to such species which involve condensation protocols. Thus, the synthesis of a complete series of oligomers takes place in a single reaction and structural control of the oligomer end groups is possible. In this paper we describe full details of our work on the synthesis, characterization, structures and electrochemistry of these and related species $\mathbf{7_2}-\mathbf{7_9}$, $\mathbf{8_2}-\mathbf{8_7}$, and $\mathbf{9_2}-\mathbf{9_7}$ (the subscript refers to the number of ferrocene units present).

Results and Discussion

Previous studies of species in which two ferrocene units are joined by a spacer group of varying length have shown that, as would be expected, as the spacer length increases the interaction between the iron sites decreases.[34] This is exemplified by a series of oligosilane spaced biferrocenes of which the simplest is diferrocenyldimethylsilane, $\mathbf{7_2}$, which was first synthesized and studied by Wrighton and co-workers.[35] For $\mathbf{7_2}$ they observed two oxidation waves with a redox coupling of 0.15 V. Pannell and Diaz have reported comparative electrochemical studies of bis(ferrocenyl)oligosilanes $Fc(SiMe_2)_xFc$ (x = 2, 3, and 6), (Fc = Fe(η-C_5H_5)(η-C_5H_4)) and found that the redox coupling and the associated interaction between the iron centers decreases with an increase in the number of silicon atoms in the spacer group.[36] For a biferrocene with the disilane spacer $Fc(SiMe_2)_2Fc$ the redox coupling was 0.11 V and for the trisilane-bridged species $Fc(SiMe_2)_3Fc$ the value was ca. 0.08

(9) Atzkern, H.; Bergerat, P.; Fritz, M.; Hiermeier, J.; Hudeczek, P.; Kahn, O.; Kanellakopulos, B.; Köhler, F. H.; Ruhs, M. *Chem. Ber.* **1994**, *127*, 277.
(10) Atzkern, H.; Hiermeier, J.; Köhler, F. H.; Steck, A. *J. Organomet. Chem.* **1991**, *408*, 281.
(11) Hmyene, M.; Yassar, A.; Escorne, M.; Percheron-Guegan, A.; Garnier, F. *Adv. Mater.* **1994**, *6*, 564.
(12) Barlow, S.; Murphy, V. J.; Evans, J. S. O.; O'Hare, D. *Organometallics* **1995**, *14*, 3461.
(13) Atzkern, H.; Bergerat, P.; Beruda, H.; Fritz, M.; Hiermeier, J.; Hudeczek, P.; Kahn, O.; Köhler, F. H.; Paul, M.; Weber, B. *J. Am. Chem. Soc.* **1995**, *117*, 997.
(14) Yamamoto, T.; Sanechika, K.; Yamamoto, A.; Katada, M.; Motoyama, I.; Sano, H. *Inorg. Chim. Acta* **1983**, *73*, 75, and references cited therein.
(15) Grimes, R. N. *Appl. Organomet. Chem.* **1996**, *10*, 209.
(16) Manners, I. *Angew. Chem., Int Ed. Engl.* **1996**, *35*, 1602 and references cited therein.
(17) Manners, I. *Chem. Br.* **1996**, *32*, 46.
(18) Brandt, P. F.; Rauchfuss, T. B. *J. Am. Chem. Soc.* **1992**, *114*, 1926.
(19) Foucher, D. A.; Tang, B. Z.; Manners, I. *J. Am. Chem. Soc.* **1992**, *114*, 6246.
(20) For the first synthesis of poly(ferrocenylphosphines) via condensation routes, see: Withers, H. P.; Seyferth, D.; Fellmann, J. D.; Garrou, P. E.; Martin, S. *Organometallics* **1982**, *1*, 1283.
(21) Manners, I. *J. Inorg. Organomet. Polym.* **1993**, *3*, 185.
(22) Foucher, D. A.; Honeyman, C. H.; Nelson, J. M.; Tang, B. Z.; Manners, I. *Angew. Chem., Int. Ed. Engl.* **1993**, *32*, 1709.
(23) Nguyen, M. T.; Diaz, A. F.; Dement'ev, V. V.; Pannell, K. H. *Chem. Mater.* **1993**, *5*, 1389.
(24) Compton, D. L.; Rauchfuss, T. B. *Organometallics* **1994**, *13*, 4367.
(25) Foucher, D. A.; Ziembinski, R.; Peterson, R.; Pudelski, J.; Edwards, M.; Ni, Y.; Massey, J.; Jaeger, R.; Vancso, G. J.; Manners, I. *Macromolecules* **1994**, *27*, 3992.
(26) Compton, D. L.; Brandt, P. F.; Rauchfuss, T. B.; Rosenbaum, D. F.; Zukoski, C. F. *Chem. Mater.* **1995**, *7*, 2342.
(27) Manners, I. *Adv. Organomet. Chem.* **1995**, *37*, 131 and references cited therein.
(28) Smith, T. W.; Kuder, J. E.; Wychick, D. *J. Polym. Sci.* **1976**, *14*, 2433.
(29) Nelson, J. M.; Rengel, H.; Manners, I. *J. Am. Chem. Soc.* **1993**, *115*, 7035.
(30) Nelson, J. M.; Lough, A. J.; Manners, I. *Angew. Chem. Int. Ed. Engl.* **1994**, *33*, 989.
(31) Seyferth and co-workers have reported that phosphorus-bridged [1]-ferrocenophane Fe(η-C_5H_4)$_2$PPh yields short chain oligomers with 2−5 ferrocene units on treatment with Fe(η-$C_5H_4PPh_2$)(η-C_5H_4Li). Attempts to achieve ROP by use of small quantities of anionic initiator were, however, unsuccessful (see ref 20).
(32) Rulkens, R.; Lough, A. J.; Manners, I. *J. Am. Chem. Soc.* **1994**, *116*, 797.
(33) Reaction of the silicon-bridged [1]ferrocenophane **5** with small amounts of anionic initiators yields living poly(ferrocenylsilanes). See Ni, Y.; Rulkens, R.; Manners, I. *J. Am. Chem. Soc.* **1996**, *118*, 4102 and references cited therein.
(34) Morrison, W. H.; Krogsrud, S.; Hendrickson, D. N. *Inorg. Chem.* **1973**, *12*, 1998.
(35) Bocarsly, A. B.; Walton, E. G.; Bradeley, M. G.; Wrighton, M. S. *J. Electroanal. Chem. Interfacial Electrochem.* **1979**, *100*, 283.
(36) Dement'ev, V. V.; Cervantes-Lee, F.; Parkanyi, L.; Sharma, H.; Nguyen, T.; Diaz, A. F.; Pannell, K. H. *Organometallics* **1993**, *12*, 1983.

Scheme 2. Synthesis of Oligo(ferrocenylsilanes) $\mathbf{7}_{2-9}$, $\mathbf{8}_{2-7}$, and $\mathbf{9}_{2-7}$

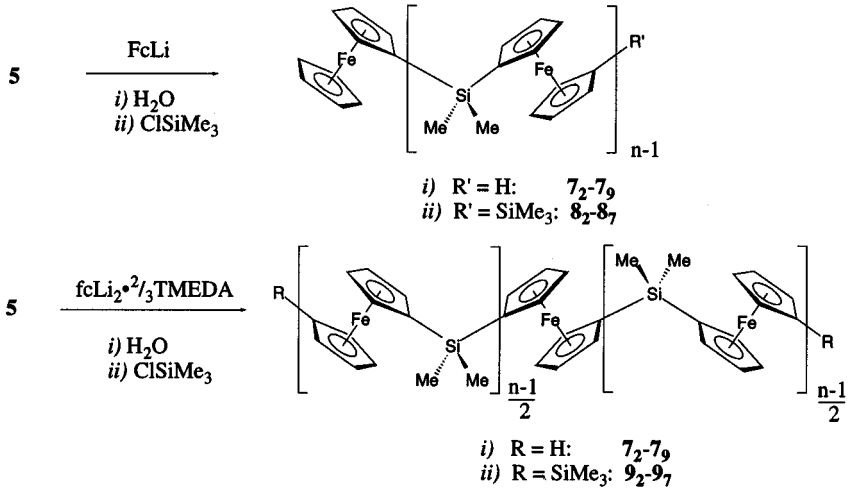

V. In the case of a hexasilane spacer only a single redox wave was detected.

There are numerous studies on other bridged biferrocene systems (e.g., Fc-Fc,[8,37] Fc-S-Fc,[38] Fc-PR-Fc,[39] Fc-CR_2-Fc,[34,39] and Fc-C_2R_4-Fc[34,39]) for which two redox couples are generally observed by cyclic voltammetry. The number of electrochemical investigations on isolated bridged oligo(ferrocenes) decreases rapidly with an increasing number of linked ferrocene units present. Reports on trinuclear ferrocene derivatives are considerably less frequent then those on bridged biferrocenes and only very few electrochemical studies have been published on linear bridged tetraferrocenes.[10,12,37,40−42] Köhler and co-workers synthesized the doubly dimethylsilyl-bridged oligo(ferrocenylsilanes) $\mathbf{10}_2$, $\mathbf{10}_3$, and $\mathbf{10}_4$ and extensively studied their redox behavior by cyclic voltammetry.[10] For the systems containing three and four iron centers they found three reversible redox processes and they suggested that oxidation of the doubly bridged tri- and tetra(ferrocenylsilanes) $\mathbf{10}_3$ and $\mathbf{10}_4$ occurs at the terminal ferrocenyl units first. Inductive effects, electrostatic interactions, superexchange, solvent effects, and electron delocalization were discussed as possible influences on the observed redox behavior of these systems. Zanello and Herberhold found that the redox behavior of chalcogen-bridged tri(ferrocenes) **11** and of combined chalcogen/perchalcogen bridged tetra(ferrocenes) **12** to be similar to that of $\mathbf{10}_3$ and $\mathbf{10}_4$ respectively.[42] Generally, bridged oligo(ferrocenes) with more then three iron centers were isolated only in milligram quantities. To our knowledge, until very recently, no reports existed on the electrochemical studies of well-defined linear oligomer systems containing more than four ferrocene units.[43,44]

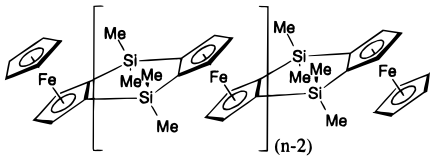

$\mathbf{10}_n$ (n = 2, 3, 4)

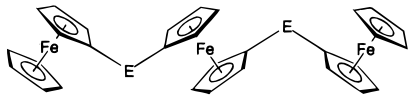

11 E = S, Se, Te

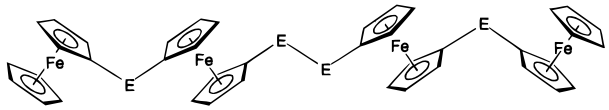

12 E = S, Se, Te

Synthesis and Isolation of the Oligo(ferrocenylsilanes) $\mathbf{7}_2-\mathbf{7}_9$, $\mathbf{8}_2-\mathbf{8}_7$, and $\mathbf{9}_2-\mathbf{9}_7$. We approached the synthesis of a range of oligo(ferrocenyldimethylsilanes) via the anionic ring-opening oligomerization of silicon-bridged [1]ferrocenophane **5** (Scheme 2). Seyferth and co-workers previously reported that a similar process operates for the phosphorus-bridged [1]ferrocenophane fcPPh to afford oligomers with between two and five ferrocene units.[31] When **5** was reacted with 1, 0.5, or 0.25 equiv of ferrocenyllithium, FcLi, or the N,N′-tetramethylethylenediamine (TMEDA) complex of 1,1′-dilithioferrocene, $fcLi_2 \cdot {}^2/_3TMEDA$, followed by quenching with water, oligo(ferrocenylsilanes) $\mathbf{7}_{2-9}$ with a Poisson distribution of molecular weights around that of the oligomer of the desired chain length were obtained.[45] Isolation of extensive series of individual well-defined oligomers was achieved by subjecting the reaction products to column chromatography on aluminum oxide that was previously deactivated with anhydrous ammonia. Applying a gradient of dichloromethane in cyclohexane varying from 10−30% resulted in the isolation of 0.25 g amounts of dimer−pentamer $\mathbf{7}_2-\mathbf{7}_5$. Higher oligomers $\mathbf{7}_6-\mathbf{7}_9$ could be obtained pure in 50−100 mg quantities after repeated chromatography and collection of the fractions of high purity only. Purity was checked by observation of a single spot by TLC. The absence of higher oligomer impurities was also verified by mass spectrometry. Due to depolymerization under the conditions necessary to observe the molecular ion, peaks for lower molecular weight species were detected for all of the oligomers.[46] The oligomers $\mathbf{8}_2-\mathbf{8}_7$ and $\mathbf{9}_2-\mathbf{9}_7$ were prepared analogously (Scheme 2) and were similarly purified and characterized.

(37) Brown, G. M.; Meyer, T. J.; Cowan, D. O.; LeVanda, C.; Kaufman, F.; Roling, P. V.; Rausch, M. D. *Inorg. Chem.* **1975**, *14*, 506.

(38) O'Connor Salazar, D. C.; Cowan, D. O. *J. Organomet. Chem.* **1991**, *408*, 227.

(39) Kotz, J. C.; Nivert, C. L.; Lieber, J. M.; Reed, R. C. *J. Organomet. Chem.* **1975**, *91*, 87.

(40) Atzkern, H.; Huber, B.; Köhler, F. H.; Müller, G.; Müller, R. *Organometallics* **1991**, *10*, 238.

(41) Delgado-Pena, F.; Talham, D. R.; Cowan, D. O. *J. Organomet. Chem.* **1983**, *253*, C43-C46.

(42) Zanello, P.; Opromolla, G.; Herberhold, M.; Brendel, H.-D. *J. Organomet. Chem.* **1994**, *484*, 67.

(43) Seyferth *et. al.* reported on the isolation of a pentaferrocenylphosphine, but no electrochemical studies on this compound were reported. (see ref 20).

(44) After this manuscript was submitted, Nishihara and co-workers reported studies of a series of hexyl-substituted oligo(ferrocenes) Fc-$(fc)_{n-2}$-Fc ($n = 2-6$). See: T. Hirao, M. Kurashima, K. Aramaki, H. Nishihara, *J. Chem. Soc., Dalton Trans.* **1996**, 2929.

Table 1. Melting Points of Oligomers $\mathbf{7}_2-\mathbf{7}_9$, $\mathbf{9}_2-\mathbf{9}_7$, and High Polymer **6**

oligomer	mp/°C	oligomer	mp/°C
$\mathbf{7}_2$	97−98	$\mathbf{9}_2$	
$\mathbf{7}_3$	146	$\mathbf{9}_3$	67−68
$\mathbf{7}_4$	117−118	$\mathbf{9}_4$	87−89
$\mathbf{7}_5$	172	$\mathbf{9}_5$	118
$\mathbf{7}_6$	136−137	$\mathbf{9}_6$	124−126
$\mathbf{7}_7$	146−147	$\mathbf{9}_7$	131
$\mathbf{7}_8$	140−142		
$\mathbf{7}_9$	152−153		
6[a]	135[b], 122[c]		

[a] Measured by DSC. [b] $M_w = 1.2 \times 10^4$, $M_n = 1.1 \times 10^4$. [c] $M_w = 5.2 \times 10^5$, $M_n = 3.4 \times 10^5$.

Physical Properties of the Oligo(ferrocenylsilanes) $\mathbf{7}_2-\mathbf{7}_9$, $\mathbf{8}_2-\mathbf{8}_7$, and $\mathbf{9}_2-\mathbf{9}_7$. All the oligo(ferrocenylsilanes) studied are air-stable amber colored compounds. $\mathbf{7}_2$, $\mathbf{7}_3$ and $\mathbf{7}_5$ are highly crystalline and the structures of $\mathbf{7}_3$ and $\mathbf{7}_5$ were determined by single crystal X-ray diffraction.[32,45,47,48] $\mathbf{7}_4$, $\mathbf{7}_6$, and $\mathbf{7}_7$ were microcrystalline compounds and $\mathbf{7}_8$ and $\mathbf{7}_9$ were isolated as amber powders. The oligo(ferrocenylsilanes) are soluble in aromatic solvents, dichloromethane, THF and diethyl ether, but the higher oligomers are insoluble in very polar solvents such as acetonitrile or acetone. The solubility of the oligomers in non-polar solvents such as hexanes and pentane decreases with chain length and is generally lower for oligomers containing an odd number of ferrocene groups. The melting points of the oligo(ferrocenylsilanes) $\mathbf{7}_2-\mathbf{7}_9$ are given in Table 1. Notably the melting points of $\mathbf{7}_3$, $\mathbf{7}_5$, $\mathbf{7}_7$, and $\mathbf{7}_9$ are higher then those of $\mathbf{7}_2$, $\mathbf{7}_4$, $\mathbf{7}_6$, and $\mathbf{7}_8$. Both series converge to a melting point of ca. 145 °C, which is slightly higher then that of high polymer **6** ($M_n = 340\,000$) for which a melting point of 122°C was found by differential scanning calorimetry (DSC).[27] For the trimethylsilyl terminated oligo(ferrocenylsilane) series, $\mathbf{9}_2$ is an oil at room temperature whereas a gradual increase of the melting points from 67−68 °C for trimer $\mathbf{9}_3$ to 131 °C for heptamer $\mathbf{9}_7$ was detected which reflects the effect of the trimethylsilyl end groups.

Characterization of the Oligo(ferrocenylsilanes) $\mathbf{7}_2-\mathbf{7}_9$, $\mathbf{8}_2-\mathbf{8}_7$, and $\mathbf{9}_2-\mathbf{9}_7$. All oligo(ferrocenylsilanes) were characterized by ^{1}H, ^{13}C, and ^{29}Si NMR spectroscopy and in all spectra separate signals could be observed and assigned to end groups. This effect is most clearly shown by the ^{29}Si NMR spectra of $\mathbf{8}_2-\mathbf{8}_7$ (Figure 1) where resonances for the $FcSiMe_2$ end group (at −6.6 ppm) represents the site of ferrocenyllithium initiated ring opening oligomerization and the $SiMe_3$ signal (at −3.1 ppm) is assigned to the oligomer end group obtained by derivatization of the terminal η-C_5H_4Li group with $SiMe_3Cl$. An additional signal at −6.5 ppm is assigned to the interior dimethylsilyl group(s) of $\mathbf{8}_3-\mathbf{8}_7$. For $\mathbf{7}_2-\mathbf{7}_9$ a ^{29}Si resonance corresponding to the ferrocenyldimethylsilyl end groups was observed and, for oligomers $\mathbf{7}_4-\mathbf{7}_9$ an additional resonance only ca. 0.2 ppm further downfield was assigned to the interior dimethylsilyl group(s). All oligo(ferrocenylsilanes) $\mathbf{9}_2-\mathbf{9}_7$ show a signal for the terminal $SiMe_3$ groups and one for the interior $SiMe_2$ group(s). Generally as the oligomer chain length increases, the intensity of the signal for the interior $SiMe_2$ groups increases compared to those for the end groups (see Figure 1).

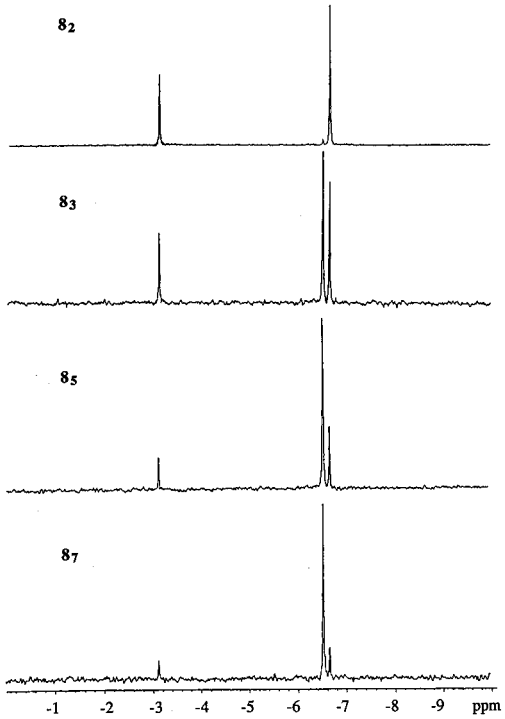

Figure 1. ^{29}Si NMR spectra of $\mathbf{8}_2$, $\mathbf{8}_3$, $\mathbf{8}_5$, and $\mathbf{8}_7$ (in $CDCl_3$).

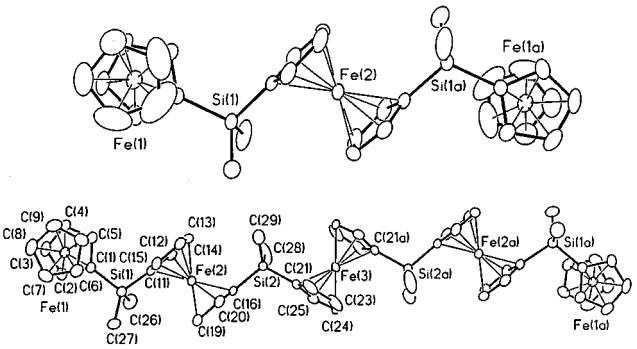

Figure 2. Molecular structures of trimer $\mathbf{7}_3$ (top) and pentamer $\mathbf{7}_5$ (bottom).

End groups could also be identified in the ^{1}H NMR spectra (at 4.07−4.09 ppm for the terminal η-C_5H_5 ligand of $\mathbf{7}_2-\mathbf{7}_9$ and $\mathbf{8}_2-\mathbf{8}_7$ and at 0.21 ppm for the terminal $SiMe_3$ groups of $\mathbf{8}_2-\mathbf{8}_7$ and $\mathbf{9}_2-\mathbf{9}_7$). The effect of the η-C_5H_5 end group on the proton NMR shifts of the η-C_5H_4 ligands further inside the oligomer chain is best exemplified by the cyclopentadienyl region of the ^{1}H NMR spectra of $\mathbf{7}_2-\mathbf{7}_9$. For the dimer $\mathbf{7}_2$ one pair of pseudotriplets for the interior η-C_5H_4 ligands was present whereas for each additional ferrocenylsilane unit of the longer oligomers $\mathbf{7}_3$ and $\mathbf{7}_4$ an additional set of pseudotriplets slightly further upfield was assigned to η-C_5H_4 groups further inside the oligomer chain. For the longer oligomer chains $\mathbf{7}_5-\mathbf{7}_9$, no additional sets of pseudotriplets could be resolved. Similar end group effects were noted in the cyclopentadienyl region of the ^{13}C NMR spectra. For example, for the trimer $\mathbf{9}_3$ three pairs of resonances assigned to the inequivalent η-C_5H_4 ligands were observed.

X-ray Structure of the Linear Penta(ferrocenylsilane) $\mathbf{7}_5$: Analogy to the Poly(ferrocenylsilane) High Polymer 6. The oligo(ferrocenylsilanes) are useful model compounds for the high polymer, not only in regard to their electrochemical properties (vide infra), but also for their morphological characteristics. Single crystals of $\mathbf{7}_3$ and of $\mathbf{7}_5$ suitable for X-ray structure determination were obtained. The structure of $\mathbf{7}_3$ has been previously described and, for comparative purposes, is

(45) Subsequent to our report of the synthesis of the linear trimer $\mathbf{7}_3$ by ring-opening oligomerization of **5** (ref 32) the synthesis of this species via an alternative route involving the reaction of $fcLi_2$ with $FcSiMe_2Cl$ was reported: see ref 47.

(46) Pudelski, J. K.; Rulkens, R.; Foucher, D.; Lough, A. J.; Macdonald, P. M.; Manners, I. *Macromolecules* **1995**, *28*, 7301.

(47) Pannell, K. H.; Dementiev, V. V.; Li, H.; Cervantes-Lee, F.; Nguyen, M. T.; Diaz, A. F. *Organometallics* **1994**, *13*, 3644.

(48) Lough, A. J.; Manners, I.; Rulkens, R. *Acta Crystallogr.* **1994**, *C50*, 1667.

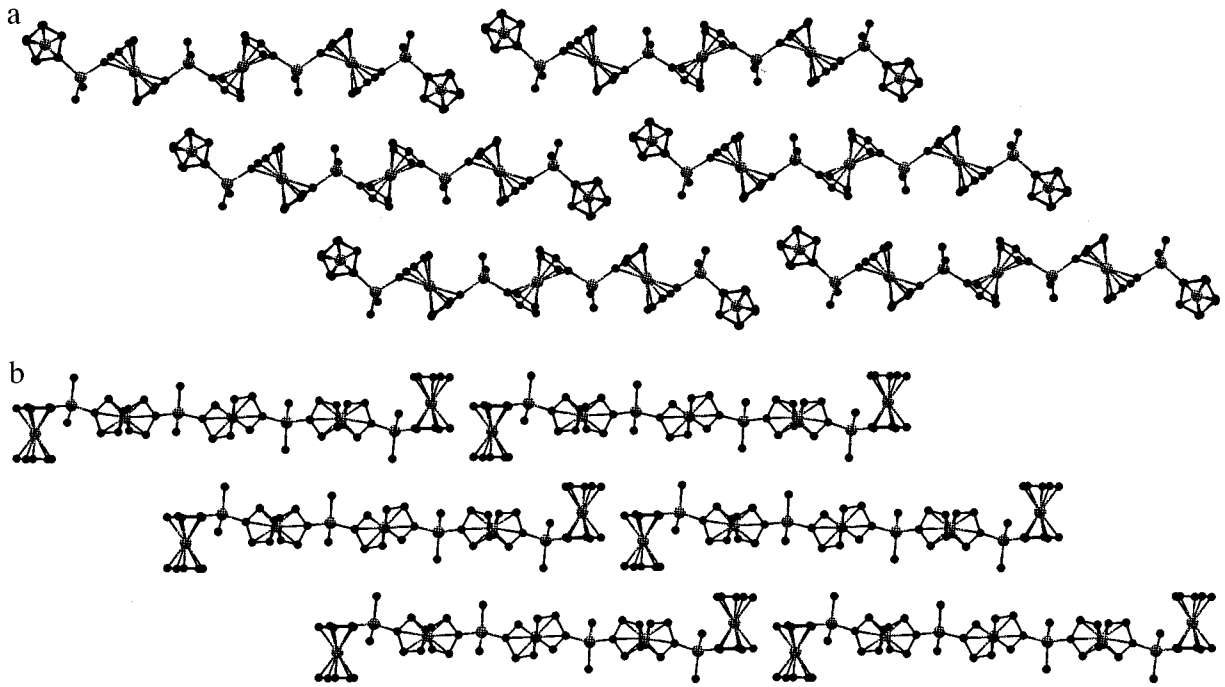

Figure 3. Views of the crystal packing arrangement of $\mathbf{7_5}$. (a) Top view of a layer of molecules parallel to the [0 1 1] plane. (b) View perpendicular to that of (a) showing three pairs of molecules in three [0 1 1] planes.

shown in Figure 2, together with the molecular structure of $\mathbf{7_5}$.[49] A summary of selected crystallographic data for $\mathbf{7_5}$ is given in Table 5 and selected bond length and angles are given in Table 6a. For both $\mathbf{7_3}$ and $\mathbf{7_5}$, the terminal ferrocenyl groups are twisted in opposite directions perpendicular to the interior ferrocenyl unit(s).[50] The *intra*molecular distances between iron atoms of neighboring ferrocenes for $\mathbf{7_3}$ are 6.187(4) Å and for $\mathbf{7_5}$ Fe(1)···Fe(2) = 6.056(5) Å and Fe(2)···Fe(3) = 6.913(5) Å. Remarkably, closer *inter*molecular iron-iron distances are present for both $\mathbf{7_3}$ and $\mathbf{7_5}$; the distance between iron atoms of terminal ferrocenes of two neighboring molecules are 5.828(3) Å for $\mathbf{7_3}$ and 5.663(4) Å for $\mathbf{7_5}$. Based on molecular mechanics calculations, the perpendicular orientation of the ferrocenyl end groups of $\mathbf{7_3}$ and $\mathbf{7_5}$ allows close intermolecular contacts between the cyclopentadienyl ligands and the iron atoms which were found to stabilize the lattice through favourable electrostatic interactions.[51] The central -fc-$SiMe_2$-fc-$SiMe_2$-fc- unit of $\mathbf{7_5}$ is close to a trans planar zigzag conformation with the adjacent ferrocenyl groups oriented ca. 110° relative to one another.[50]

The powder X-ray diffraction pattern of oligo(ferrocenylsilane) $\mathbf{7_5}$ was previously compared with that of high polymer **6** and we established that the molecular structure of $\mathbf{7_5}$ is an excellent model for the structure of crystalline domains of **6**.[52] Thus the strongest reflection of the X-ray powder diffractogram has been assigned to planes with [0 1 1] Miller indices. A top view of a [0 1 1] plane of $\mathbf{7_5}$ is shown in Figure 3a. The presence of the iron atoms of the pentamer molecular chain in these planes causes the strong intensity of the [0 1 1] diffraction peak in the X-ray powder diffractogram. A polymer structure consisting of parallel linear chains in which the ferrocenylsilane units possess a zigzag trans configuration can be easily envisaged by substituting two closely neighbored ferrocenyl end groups by a connecting ferrocene unit.[51] Figure 3b presents a view perpendicular to that in Figure 3a and shows three pairs of molecules from three different [0 1 1] planes. The layer distance between these planes appears to be determined by the methyl substituents on the silicon atoms which are oriented above and below the [0 1 1] planes. The d-spacing of 6.287 Å is comparable to that found for the strongest reflection found in the powder X-ray diffractogram of high molecular weight poly(ferrocenylsilane) **6** (6.37 Å). Interestingly, the most intense reflection found in the powder X-ray diffraction pattern of the very recently synthesized dihydro-substituted poly(ferrocenylsilane) **13** corresponds to a d-spacing of 5.87 Å.[46] Thus the shorter Si-H bond length and the small covalent radius for the hydrogen substituents allows a 0.50 Å closer spacing between "layers" of polymer chains of **13** compared to those of **6**.

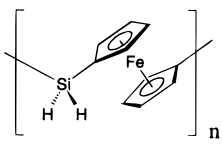

13

Electrochemical Studies of the Oligo(ferrocenylsilanes) $\mathbf{7_2}$ −$\mathbf{7_9}$. In order to gain further insight into the electrochemical behavior of poly(ferrocenes) such as **4** and **6**, the electrochemical properties of the oligo(ferrocenylsilanes) were studied in detail. The electrochemical behavior of this series of oligomers was investigated by cyclic voltammetry (CV), differential pulse voltammetry (DPV) and chronoamperometry. The solvent often preferred for the oxidation of ferrocenes is dichloromethane due to its inertness towards ferrocenium-type ions. However, because of the tendency of the oligomer oxidation products to

(49) The X-ray structure of $\mathbf{7_3}$ has been independently reported previously by ourselves (see ref 48) and by Pannell et. al. (see ref 47).

(50) The exact conformation of oligo(ferrocenylsilanes) $\mathbf{7_x}$ is defined by three torsion angles ϕ, ψ and χ for which a definition can be found in ref 51b. For $\mathbf{7_3}$ $\phi_1 = -\phi_2 = 74°$, $\psi_1 = -\psi_2 = 179°$ and $\chi = 180°$; for $\mathbf{7_5}$ $\phi_1 = -\phi_4 = -74°$, $\phi_2 = -\phi_3 = 167°$, $\psi_1 = -\psi_4 = 174°$, $\psi_2 = -\psi_2 = 179°$, $\chi_1 = -\chi_3 = 159°$ and $\chi_2 = 180°$; for $\mathbf{7_3}^{2+}$ $\phi_1 = -169°$, $\psi_1 = 172°$, $\chi = 152°$, $\psi_2 = 170°$ and $\phi_2 = -158°$. For a perfect trans planar zigzag conformation all angles ϕ, ψ, and χ would be 180°.

(51) A molecular mechanics study of oligo(ferrocenylsilanes) $\mathbf{7_2}$, $\mathbf{7_3}$, and $\mathbf{7_5}$ utilizing the new generalized Extensible Systematic Force Field (ESFF) program was recently reported by O'Hare et al. They suggest that some ferrocene units in a polymer chain of **6** may be twisted perpendicular to the layers in the same manner as the terminal ferrocenes in the structure of $\mathbf{7_5}$. See: (a) Barlow, S.; Rohl, A. L.; O'Hare, D. *J. Chem. Soc. Chem. Commun.* **1996**, 257. (b) Barlow, S.; Rohl, A. L.; Shi, S.; Freeman, C. M.; O'Hare, D. *J. Am. Chem. Soc.* **1996**, *118*, 7578.

(52) Rasburn, J.; Petersen, R.; Jahr, T.; Rulkens, R.; Manners, I.; Vancso, G. J. *Chem. Mater.* **1995**, *7*, 871.

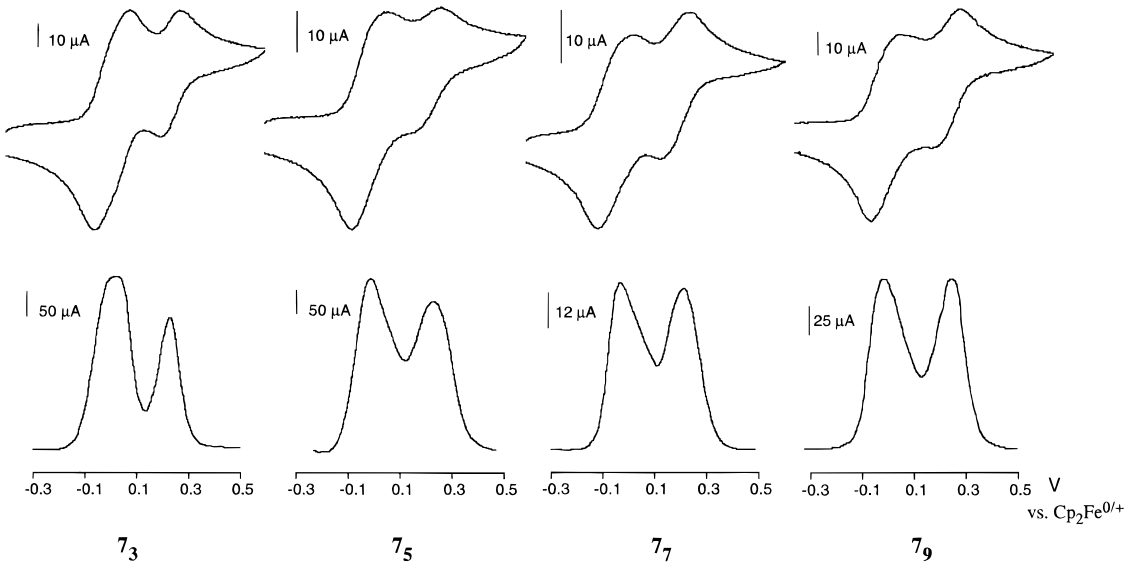

Figure 4. Cyclic voltammograms (top row) and differential pulse voltammograms (bottom row) of oligo(ferrocenylsilanes) with an odd number of iron atoms.

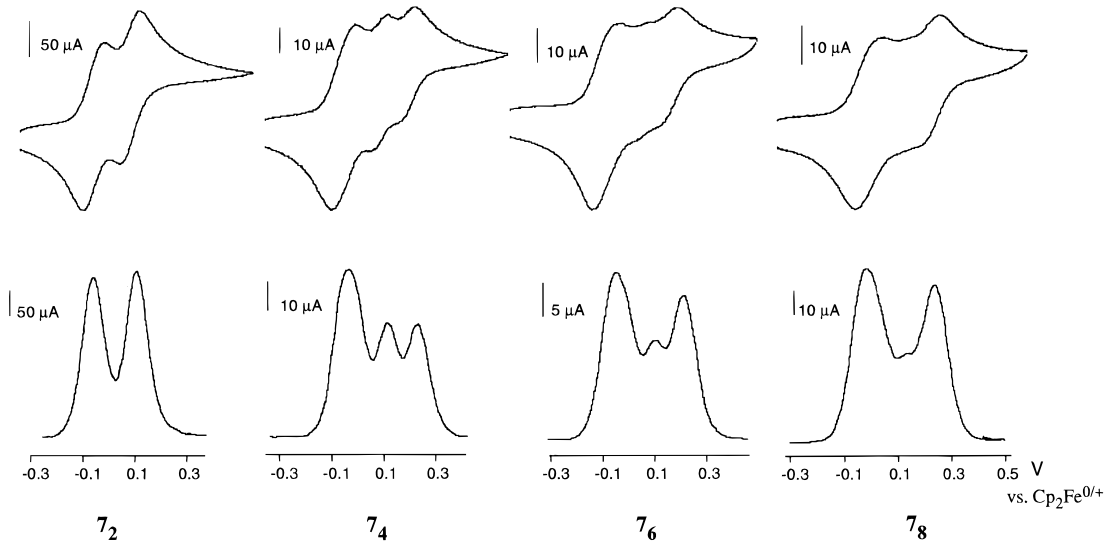

Figure 5. Cyclic voltammograms (top row) and differential pulse voltammograms (bottom row) of oligo(ferrocenylsilanes) with an even number of iron atoms.

Table 2. Cyclic Voltammetric Data of Oligo(ferrocenylsilane)s $\mathbf{7_2}-\mathbf{7_9}$[c]

oligomer[a]	$E^1_{1/2}$	$E^2_{1/2}$	$E^3_{1/2}$	$E^2_{1/2} - E^1_{1/2}$	$E^3_{1/2} - E^1_{1/2}$
$\mathbf{7_2}$	−0.02	0.13		0.15	
$\mathbf{7_3}$	−0.01[b]	0.21		0.22	
$\mathbf{7_4}$	−0.02	0.13	0.24	0.15	0.26
$\mathbf{7_5}$	0.00[b]	0.22		0.22	
$\mathbf{7_6}$	−0.01	0.12	0.23	0.13	0.24
$\mathbf{7_7}$	0.00	0.22		0.22	
$\mathbf{7_8}$	−0.02	0.11	0.22	0.13	0.24
$\mathbf{7_9}$	0.00	0.21		0.21	

[a] Cyclic voltammograms of $\mathbf{8_2}-\mathbf{8_7}$ and $\mathbf{9_2}-\mathbf{9_7}$ were identical to those of $\mathbf{7_2}-\mathbf{7_7}$, respectively. [b] Two overlapping waves. [c] All values in volt vs $[Fe(\eta\text{-}C_5H_5)_2]^{0/+}$.

form films on the electrode surfaces in this solvent, we employed a solvent mixture of 1:1 CH_2Cl_2:CH_3CN for all of our electrochemical studies. For all oligomers $\mathbf{7_2}-\mathbf{7_9}$ a plot of peak current vs $\nu^{1/2}$ was linear, indicating diffusion controlled redox processes (ν = scan rate). Results on the electrochemical behavior of oligo(ferrocenylsilanes) $\mathbf{7_2}-\mathbf{7_9}$ are presented in Figures 4 and 5, Tables 2 and 3 and are explained in Schemes 3 and 4.

A. General Behavior and Results for Diferrocenylsilane $\mathbf{7_2}$. Results for $\mathbf{7_2}$ were consistent with the occurrence of two essentially Nernstian one-electron oxidations to stable products (eq 1).

$$\mathbf{7_2} \overset{E^1_{1/2}}{\rightleftharpoons} \mathbf{7_2}^{+} \overset{E^2_{1/2}}{\rightleftharpoons} \mathbf{7_2}^{2+} \quad (1)$$

Table 3. Formal Potentials of Polynuclear Complexes $\mathbf{7_2}-\mathbf{7_9}$ Measured by Differential Pulse Voltammetry[a,f]

complex	$E^{1a}{}_{1/2}$[b]	$E^{1b}{}_{1/2}$	$E^2_{1/2}$	$E^3_{1/2}$	$(E^{max}{}_{1/2} - E^{1a}{}_{1/2})$[c] (V)
$\mathbf{7_2}$	0.013(1)		0.169(1)		0.156
$\mathbf{7_3}$	0.008(1)[d]	0.068(1)[d]	0.261(1)		0.253
$\mathbf{7_4}$	−0.021(1)[d]	0.029(1)[d]	0.152(1)	0.270(1)	0.291
$\mathbf{7_5}$	−0.010(2)	ca. 0.06(1)[e]	0.236(2)		0.246
$\mathbf{7_6}$	−0.003(3)		0.150(1)	0.248(2)	0.251
$\mathbf{7_7}$	−0.022(3)	ca. 0.06(1)[e]	0.240(3)		0.262
$\mathbf{7_8}$	0.008(4)		0.158(1)	0.268(3)	0.260
$\mathbf{7_9}$	0.002(5)		0.272(4)		0.270

[a] Symbolism: $E^m{}_{1/2}(n)$: potential of mth wave having stoichiometry of n electrons. [b] Calculated from peak potential using $E_{1/2} = E_{pk}$ − pulse width/2. [c] Separation between most positive and most negative $E_{1/2}$ values. [d] Separation of $E^{1a}{}_{1/2}$ and $E^{1a}{}_{1/2}$ calculated from simulations and from peak broadening according to ref 55. [e] Estimated from unresolved shoulder. [f] All values in V vs $[Fe(\eta\text{-}C_5H_5)_2]^{0/+}$.

Scheme 3. Redox Behavior of "odd" Oligomers $\mathbf{7_3}$, $\mathbf{7_5}$, $\mathbf{7_7}$, and $\mathbf{7_9}$[a]

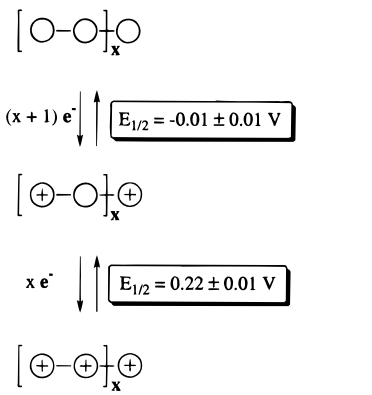

[a] $E_{1/2}$ values given vs ferrocene/ferrocenium.

Scheme 4. Redox Behavior of "even" Oligomers $\mathbf{7_2}$, $\mathbf{7_4}$, $\mathbf{7_6}$, and $\mathbf{7_8}$[a]

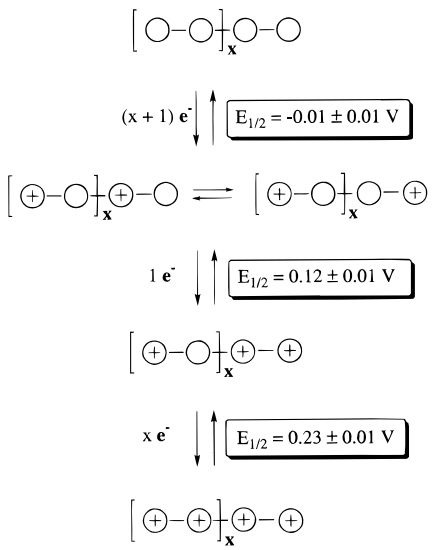

[a] $E_{1/2}$ values given vs ferrocene/ferrocenium.

This dinuclear complex was the only system for which cyclic voltammetry gave visually unambiguous results (Figure 5, left). Formal potentials of −0.02 V and 0.13 V were obtained for $E^1{}_{1/2}$ and $E^2{}_{1/2}$, respectively (Table 2). The potential difference of 0.15 V for $\Delta E_{1/2}$ ($\Delta E_{1/2} = E^2{}_{1/2} - E^1{}_{1/2}$) is typical of ferrocenyl moieties experiencing weak to moderate level electronic interactions (vide infra). Chronoamperometry at a planar Pt disk confirmed that both oxidations were chemically reversible. A diffusion coefficient of 1.5×10^{-5} cm^2/s (assuming $n = 2$ e$^-$) was obtained from the Cottrell constants[53] when the applied potential was stepped positive of the second oxidation.

Differential pulse voltammetry of $\mathbf{7_2}$ at a Pt disk showed the expected pair of symmetric waves of equal height (Figure 5, bottom left). Peak widths at half-height ($W_{1/2}$) were ca. 95 mV when the pulse amplitude was low (10 mV), close to the theoretical value of ca. 90 mV for $n = 1$ at 298 K.[54] $W_{1/2}$ increased slightly with larger pulse amplitudes, but all one-electron waves for this and heavier homologues displayed widths of 110 mV or less. The well-behaved pulse voltammetry of the series was advantageous in defining the electrochemical response of several members of the series which displayed highly overlapped CV curves.

(53) Cottrell constant $= it^{1/2} = 1.77nFAD^{1/2}C^*$, where F is the Faraday constant, A is electrode area, and D and C^* are the diffusion coefficient and bulk concentration, respectively, of the electrochemical reactant.

(54) Parry, E. P.; Osteryoung, R. A. *Anal. Chem.* **1964**, *37*, 1634.

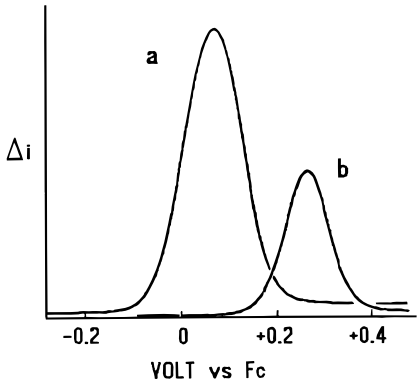

Figure 6. Digitally simulated DPV responses modeling threecouple response of $\mathbf{7_3}$. (Curve a: $E^{1a}{}_{1/2} = +0.025$ V, $E^{1b}{}_{1/2} = +0.085$ V; curve b: $E^2{}_{1/2} = +0.248$ V. For all couples $k_s = 10^{-2}$ cm/s, $a = 0.5$. Other parameters: pulse time 50 ms, pulse width 10 s, pulse height 10 ms, scan rate 5 mV/s. Compare with experimental response of $\mathbf{7_3}$ in Figure 4.)

B. Trinuclear $\mathbf{7_3}$ and Other "Odd" Oligomers. Two DPV peaks were also observed for the trinuclear complex $\mathbf{7_3}$. The integration value of the first peak was about twice that of the second. The first peak was broader than the second by about 33 mV, suggesting that two unresolved one-electron processes were responsible, differing by ca. 60 mV in potential.[55] Digital simulations confirmed this conclusion. Figure 6 shows a simulation based on two one-electron processes separated by 60 mV (trace a) superimposed on one for the well-separated one-electron oxidation assigned to $\mathbf{7_3}^{2+/3+}$ which appeared at $E^2{}_{1/2} = 0.261$ V.[56]

This pattern of two waves of different size held for the entire set of complexes containing an odd number of iron atoms (Figure 4, Scheme 3). Integration of the peak areas (proportional to the charges passed) for the first:second waves established ratios of 2:1 for $\mathbf{7_3}$, 3:2 for $\mathbf{7_5}$, 4:3 for $\mathbf{7_7}$, and 5:4 for $\mathbf{7_9}$. As discussed below, this pattern is consistent with a model in which the initial oxidation occurs at every other Fe center. The ratio converges toward 1:1 for long oligomer chains, a conclusion confirmed by the behavior of the high polymer **6**.[19,27]

The separation of the $E_{1/2}$ potentials contributing to the first wave of $\mathbf{7_5}$ was estimated from the broadening of the DPV peak[55] as $\Delta E_{1/2} = 70$ mV (Scheme 5, Table 3). The complexities of the first waves of $\mathbf{7_7}$ (four electrons) and $\mathbf{7_9}$ (five electrons) precluded more precise analyses; we are simply able to say that the three (or five) one-electron couples occur at very similar potentials in the first waves of the two longest-chain odd oligomers.

Our results on the trinuclear complex $\mathbf{7_3}$ are sufficiently different from those of Pannell and co-workers[47] to warrant a comment. These workers found a greater wave separation between $E^{1a}{}_{1/2}$ and $E^{1b}{}_{1/2}$ for $\mathbf{7_3}$, namely $\Delta E_{1/2} = 110$ mV, compared to our 60 mV. This apparent discrepancy may be ascribed to solvent differences. The CV measurements of Pannell et. al. were performed in CH_2Cl_2. We obtained a similar finding in a 1:1 CH_2Cl_2:butyronitrile mixture (resolution of the two DPV peaks was attained), but always found a single unresolved wave when CH_3CN was the solvent or co-solvent. There appears to be a slight preferential change in solvation energy for the dication $\mathbf{7_3}^{2+}$ over that of the monocation $\mathbf{7_3}^{+}$ in CH_3CN. Acetonitrile is known to preferentially solvate polycations.[57]

(55) Richardson, D. E.; Taube, H. *Inorg. Chem.* **1981**, *20*, 1278.

(56) To obtain $E_{1/2}$ from the DPV peak potential: $E_{1/2} = E_{pk} + E_{pulse}/2$, where E_{pulse} is the pulse height (10−25 mV). With $E_{pulse} = 25$ mV, E_{pk} is 12.5 mV negative of $E_{1/2}$ for an oxidation process.

(57) see, for example Bowyer, W. J.; Geiger, W. E. J. *Electroanal. Chem.* **1988**, *239*, 253.

Scheme 5. Detailed Redox Behavior of Pentamer $\mathbf{7_5}$[a]

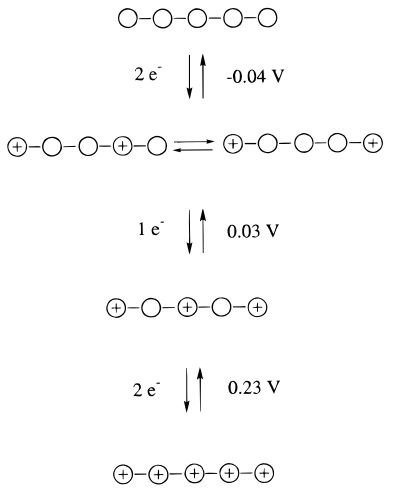

[a] $E_{1/2}$ values given vs ferrocene/ferrocenium.

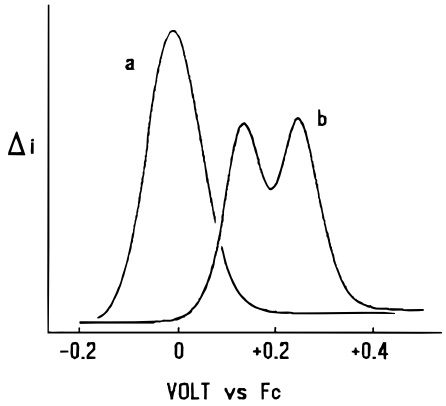

Figure 7. DPV simulations for four couple response of $\mathbf{7_4}$. (Curve a: $E^{1a}{}_{1/2} = -0.035$ V, $E^{1b}{}_{1/2} = +0.015$ V; curve b: $E^{2}{}_{1/2} = +0.140$ V, $E^{3}{}_{1/2} = +0.257$ V. Compare to experimental response of $\mathbf{7_4}$ in Figure 5.)

C. Tetranuclear $\mathbf{7_4}$ and Other "Even" Oligomers. The tetranuclear complex $\mathbf{7_4}$ has three waves integrating to a relative 2:1:1 stoichiometry. The broadening of the first wave suggested a 50 mV separation of the $E_{1/2}$ values for $\mathbf{7_4}^{0/+}$ and $\mathbf{7_4}^{+/2+}$; digital simulations based on this value reproduced the observed peak breadth (Figure 7, Scheme 4). Except for $\mathbf{7_2}$, all oligomers containing an even number of Fe centers gave a 3-wave pattern (see Figure 5). The integrated ratios of these peaks were 2:1:1 for $\mathbf{7_4}$, 3:1:2 for $\mathbf{7_6}$, and 4:1:3 for $\mathbf{7_8}$. Noteworthy is the fact that the middle wave always corresponds to a one-electron process for the even oligo(ferrocenylsilanes) (Scheme 4); as the oligomer chain increases the relative contribution of the middle wave decreases and it is barely observed for the octamer $\mathbf{7_8}$. The stoichiometry ratio converges on 1:0:1 for a long oligomer, confirming that both the even oligomers and odd oligomers extrapolate to the same electrochemical behavior viewed in the context of the high polymer **6**.

D. Significance of the Redox Patterns. The redox separation between ferrocenyl groups in $\mathbf{7_2}$ ($E^{2}{}_{1/2} - E^{1}{}_{1/2}$) is 0.15V, a value typical of moderately-interacting redox groups. A considerably larger separation (0.25 V) is found between the first and last redox processes of $\mathbf{7_3}$. This may be explained by the fact that the third oxidation of $\mathbf{7_3}$ must involve a ferrocenyl center adjacent to two previously oxidized sites. Since the inductive effects of the silyl substituents may be neglected[58] the increase in the spread of $E_{1/2}$ values is interpreted as arising from the $SiMe_2$-mediated electronic effects that increase with the number of ferrocenium groups next to the remaining iron center after the first oxidation process.

In Table 3 the quantity specified as ($E^{max}{}_{1/2} - E^{1a}{}_{1/2}$) refers to the potential separation between the first and last oxidations of the series of oligomers. For complexes involving at least three metals a value of 0.27 V ± 0.02 V is obtained for this quantity. Whatever the sequence of oxidations in the oligomers, therefore, the potential separation between the first redox process and the last is essentially constant.

The increase between the values of $\Delta E_{1/2}$ for $\mathbf{7_2}$ (0.15 V) and $\mathbf{7_9}$ (0.27 V) parallels a similar observation made earlier regarding persulfide-bridged ferrocenes.[18,59] The value of $E^{2}{}_{1/2} - E^{1}{}_{1/2}$ for di(ferrocenylpersulfide) **14** is 0.18 V, compared to a value of $\Delta E_{1/2} = 0.32$ V for the polymer **4**.

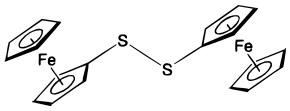

14

The voltammetry of the odd oligo(ferrocenylsilanes), and that of the high polymer, is also consistent with a model in which the first oxidation wave involves every other metal center, a very small spread of potentials (≤70 mV) being associated with the couples comprising this wave (see Scheme 5).

Analysis of the voltammetry of the even oligo(ferrocenylsilanes) is slightly more complicated than that of the odd systems (Scheme 4). For the tetranuclear complex $\mathbf{7_4}$, $x = 1$, and initial oxidation of two isolated Fe centers at the first oxidation potential results in the formation of two electronic isomers, following the earlier work by Meyer and co-workers on oligo(ferrocenylenes).[37] These isomers must be very close in energy owing to the weak Fe···Fe interactions in the complex. For both isomers a pristine Fe(II) center that has only one oxidized neighbor becomes oxidized at a slightly higher potential, leaving the remaining Fe(II) center (or centers, for higher oligomers) neighbored by two ferrocenium groups to be oxidized at the highest potential.

Spectroelectrochemical Studies

A. IR Spectroscopy of Mixed-Valent $\mathbf{7_2}^+$. Infrared spectroscopy of mixed-valent systems often gives definitive information about the phenomenon of electronic delocalization.[60] In ferrocene-based mixed valent systems a band assigned to a C-H bend of the cyclopentadienyl ring has been shown to be diagnostic of the iron oxidation state. This band shifts from 815 cm^{-1} in ferrocene to 851 cm^{-1} in ferrocenium triiodide.[5] A mixed-valent diferrocenyl complex having absorptions at both of these energies has trapped valence, whereas intrinsically delocalized systems display a single C-H frequency at close to the average of the Fe(II) and Fe(III) frequencies, i.e., ca. 830 cm^{-1}.[5,61] To our knowledge IR studies in this spectral region have been confined to solid-state samples.[5,61,62] We were interested in information about the delocalization behavior of oxidized oligo(ferrocenylsilanes) in solution, where counterion induced valence trapping[63] would be less likely. Conse-

(58) Hoh, G. L. K.; McEwen, W. E.; Kleinberg, J. *J. Am. Chem. Soc.* **1961**, *83*, 3949.

(59) Scholl, H.; Sochaj, K. *Electrochim. Acta* **1991**, *36*, 689.

(60) For leading references, see: Chin, T. T.; Lovelace, S. R.; Geiger, W. E.; Davis, C. M.; Grimes, R. N. *J. Am. Chem. Soc.***1994**, *116*, 9359.

(61) Delville, M.-H.; Rittinger, S.; Astruc, D. *J. Chem. Soc., Chem. Commun.* **1992**, 519.

(62) Dong, T.-Y.; Schei, C.-C.; Hsu, T.-L.; Lee, S.-L.; Li, S.-J. *Inorg. Chem.* **1991**, *30*, 2457.

(63) Le Narvor, N.; Lapinte, C. *Organometallics* **1995**, *14*, 634.

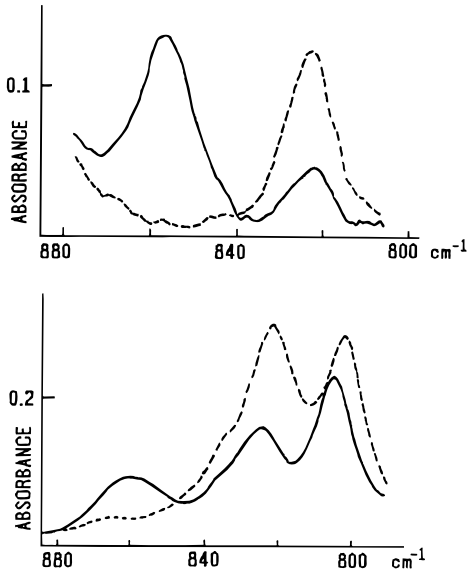

Figure 8. IR spectroelectrochemical responses in C-H bending region for oxidation of ferrocene (top) and $\mathbf{7_2}$ (bottom) (10 mM ferrocene and 17 mM $\mathbf{7_2}$ in CH_3CN/1.0 M Na[ClO_4], respectively; dotted line, before oxidation; solid line, after oxidation).

quently we obtained IR spectra of the ferrocene/ferrocenium couple and the dinuclear complex $\mathbf{7_2}/\mathbf{7_2}^+$ in thin-layer spectroelectrochemical experiments.[64] The solvent/supporting electrolyte system for these experiments was CH_3CN/0.075 M Na[ClO_4]. This medium was reasonably transparent in the spectral range of interest (780−900 cm^{-1}). Figure 8 displays results for Fe(η-C_5H_5)$_2$/[Fe(η-C_5H_5)$_2$]$^+$ (top) and $\mathbf{7_2}/\mathbf{7_2}^+$ (bottom). Oxidation of ferrocene shifts the C-H bend from 823 cm^{-1} to 857 cm^{-1}, the 34 cm^{-1} increase being consistent with that reported earlier for Fe(η-C_5H_5)$_2$/[Fe(η-C_5H_5)$_2$]$^+$ in the solid state.[5] (The small intensity band remaining at 823 cm^{-1} in Figure 8 top (solid trace) is apparently due to incomplete electrolysis). The neutral dinuclear complex $\mathbf{7_2}$ has the expected C-H band at 822 cm^{-1} and another band at 802 cm^{-1} (Figure 8, bottom). The latter is ascribed to the dimethylsilylene group since this band is absent in ferrocene but present in Fe(η-C_5H_4-$SiMe_3$)$_2$. Electrolysis to the mixed-valent monocation $\mathbf{7_2}^+$ results in absorptions at 826 cm^{-1} and 860 cm^{-1} (Figure 8, bottom, solid trace). Since a pair of bands consistent with an Fe(II)/Fe(III) system is observed, rather than a band at the Fe(II)/Fe(III) spectral average, the spectra argue strongly that on the IR time scale $\mathbf{7_2}^+$ is a trapped-valent system in solution.

B. Near-IR Spectroscopy of Mixed-Valent Oligomers with 2−5 Metals. Spectroelectrochemistry over the interval 330 nm to 2000 nm was performed on the oligomers $\mathbf{7_2}$−$\mathbf{7_5}$. Electrochemical oxidation gave rise to two important features: (1) appearance of a visible band near 620 nm assigned to ligand-to-metal charge transfer of the ferrocenium moiety[5] and (2) a near-IR band with a maximum near 1200 nm which we ascribe to an intervalence transition (IT). Figures 9 and 10 show typical experimental data and the relevant analytical data are collected in Table 4. The concentrations used to calculate the extinction coefficients in Table 4 were obtained from coulomb counts recorded during the electrolyses. Since the current efficiencies were almost certainly not 100%, the reported values of ϵ_{app} are likely to be somewhat underestimated.

The IT band of the dinuclear monocation $\mathbf{7_2}^+$ is unremarkable compared to other bis(ferrocenyl) systems which have been the subject of many investigations.[65] Its breadth at half-height is ca. 4700 cm^{-1}, consistent with the value expected from the Hush relationship[66] for trapped-valent class II[67] systems. The weak

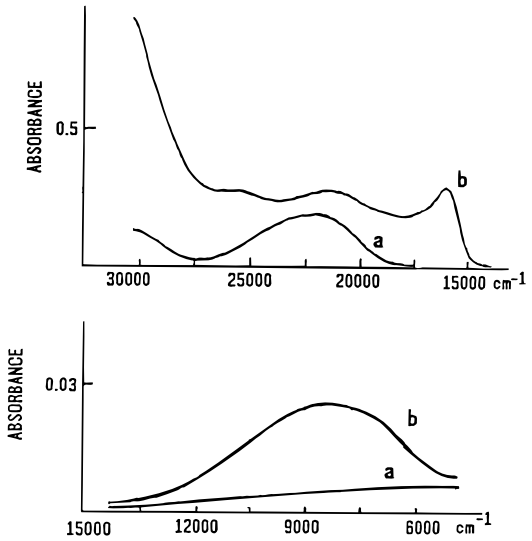

Figure 9. Optical spectroelectrochemical spectra. Top: UV-VIS region; Bottom NIR region. Curve a: prior to anodic oxidation, Curve b: after oxidation to $\mathbf{7_2}^+$.

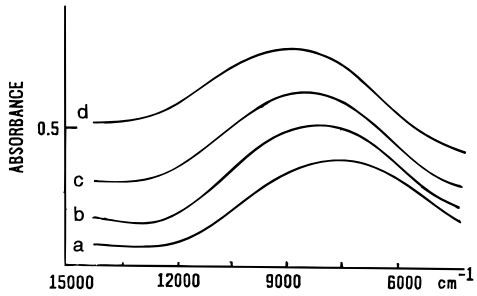

Figure 10. NIR region for spectroelectrochemical oxidation of $\mathbf{7_5}$ showing progressive shift to higher energy as oxidation proceeds. Curves a, b, c, and d recorded after passage of 1, 2, 3, and 4 faraday respectively.

Table 4. Data from Spectroelectrochemical Experiments on Oligomers $\mathbf{7_2}$−$\mathbf{7_5}$[a]

	L → M[c]		IT[d]	
oligomer[b]	$\lambda_{max} \times 10^{-3}$ cm^{-1}	ϵ_{app}[e]	$\lambda_{max} \times 10^{-3}$ cm^{-1}	ϵ_{app}[e]
$\mathbf{7_2}^+$	16.1	516	8.45	58
$\mathbf{7_3}^+$	16.1	517	8.31	56
$\mathbf{7_3}^{2+}$	16.1	877	8.45	103
$\mathbf{7_4}^+$	15.9	527	7.87	83
"$\mathbf{7_4}^{n+}$"	15.9	1360	8.68	144
$\mathbf{7_5}^+$	15.9	339	7.60	71
"$\mathbf{7_5}^{n+}$"	15.9	861	9.10	145

[a] Only data on two lowest energy bands are shown. Species shown in quotation marks reflect the uncertainty of the oxidation state distribution in the most intense spectra recorded at long electrolysis times. [b] Assigned from coulometric values during electrolysis. [c] Lowest energy visible transition is assigned as ligand-to-metal charge transfer: see ref 5. [d] Intervalence band in NIR. [e] Apparent extinction coefficient in units of M^{-1} s^{-1}.

(64) Atwood, C. G.; Geiger, W. E.; Bitterwolf, T. E. *J. Electroanal. Chem.* **1995**, *397*, 279.

(65) Recent papers containing leading references to the IT bands of biferrocenium and related ions: (a) Blackbourn, R. L.; Hupp, J. T. *J. Phys. Chem.* **1990**, *94*, 1788 (b) Sinha, U.; Lowery, M. D.; Hammack, W. S.; Hendrickson, D. N.; Drickamer, H. G. *J. Am. Chem. Soc.* **1987**, *109*, 7340.

(66) $\Delta\nu_{1/2} = (2310\ \nu_{max})^{1/2}$, where $\Delta\nu_{1/2}$ = width of IT band at half-height and ν_{max} is energy at maximum absorption. See Hush, N. S. in Progress in Inorganic Chemistry; Cotton, F. A., Ed.; John Wiley and Sons: New York, 1967; Vol 8, p 391.

(67) Robin, M. B.; Day, P. In *Advances in Inorganic Chemistry and Radiochemistry*; Emeleus, H. J., Sharpe, A. G., Eds.; Academic Press: New York, 1967; Vol. 10; p 247.

intensity IT band suggests weak metal-metal coupling; indeed, the value of the delocalization parameter α^2 calculated from this band is only 0.0004.[68] For comparison, the biferrocene cation has $\alpha^2 = 0.009$ ($\epsilon = 919$).[69]

The trinuclear monocation $\mathbf{7_3}^+$ has an IT band similar to $\mathbf{7_2}^+$ in energy and extinction coefficient; this transition has almost double the intensity in the trinuclear dication $\mathbf{7_3}^{2+}$ (Table 4). Quantitations of ϵ were more difficult with longer-chain oligomers. Ideally, the distribution of oxidized species, i.e. the concentrations of mono-, di-, trications, etc., can be obtained from knowledge of the number of coulombs passed in the optically-transparent thin layer electrode (OTTLE) cell. The coulomb counts were generally higher than expected, however, probably owing to some regeneration of the next lower oxidation state by reaction of a multiply-oxidized complex with adventitious nucleophiles. In the electrolyses of $\mathbf{7_4}$ and $\mathbf{7_5}$, therefore, we compare the spectra of the monocations with those of the most highly oxidized states as monitored by NIR spectroscopy. The latter are designated as "$\mathbf{7_m}^{n+}$" in Table 4, where $m = 4$ or 5. An interesting observation that arises from the NIR spectroelectrochemistry on $\mathbf{7_3}$, $\mathbf{7_4}$, and $\mathbf{7_5}$ is that the IT band shifts to higher energy as the degree of oxidation of the complex increases. An example of this is seen in Figure 10, which presents the NIR spectra of $\mathbf{7_5}$ as it is progressively oxidized. The energy shift of the band maximum from its first appearance ($\mathbf{7_5}^+$) at ca. 7500 cm^{-1} to its greatest intensity ($\mathbf{7_5}^{n+}$) at ca. 9000 cm^{-1} is ca. 1500 cm^{-1}. Since the IT bands are a composite of absorptions from species of different charge (and as different electronic isomers)[37] a detailed analysis is impossible. It appears certain, though, that the IT bands in the more highly oxidized forms of the complexes lie at slightly higher energies than that of the monocation. The amount of this shift appeared to be proportional to the number of oxidized metals in the oligomer.

X-ray Structure of the Mixed-Valence Dicationic Trimer $[\mathbf{7_3}]^{2+}$. In order to get additional evidence for the concept of initial oxidation of alternating iron centers of oligo(ferrocenylsilanes) and poly(ferrocenylsilanes), we attempted to obtain single crystals of a partially oxidized oligo(ferrocenylsilane). The diffusion-controlled reaction of $\mathbf{7_3}$ with three equiv of iodine in CH_2Cl_2/cyclohexane (1:5) resulted in the direct formation of X-ray quality single crystals of mixed-valent triferrocenylsilane $[\mathbf{7_3}]^{2+}[I_3]^-_2$. A summary of selected crystallographic data is given in Table 5 and selected bond length and angles are given in Table 6b. The molecular structure of $[\mathbf{7_3}]^{2+}$ $[I_3]^-_2$ (Figure 11) differs significantly from that of the neutral analog $\mathbf{7_3}$ (see Figure 2) in which the terminal ferrocene moieties are oriented in opposite directions and perpendicular to the central ferrocene unit. Indeed, it resembles the central -fcSiMe$_2$fcSiMe$_2$fc- portion of pentamer $\mathbf{7_5}$ (see Figure 2), in which the ferrocene units also obtain a planar zigzag trans conformation.[50] Thus the terminal ferrocenium groups of $[\mathbf{7_3}]^{2+}$ are positioned at a maximum separation, which is the lowest energy conformation due to the coulombic repulsion of the two positively charged centers.[70] The molecular structure of $[\mathbf{7_3}]^{2+}$ confirms that the terminal ferrocene units are oxidized in the first oxidation process of $\mathbf{7_3}$. This is shown by the average iron-cyclopentadienyl ring centroid distance, *d*(Fe-RC) which is an average of 1.692(10) Å for the terminal iron atoms, typical for that of ferrocenium species and larger then the average Fe-RC distance of the central iron atom of $[\mathbf{7_3}]^{2+}$ which is 1.630 (10) Å, typical for a pristine ferrocene center. For comparison, *d*(Fe-RC) is 1.705(6) Å for $[Fe(\eta\text{-}C_5H_4SiMe_3)_2]^+$ $[AlCl_4]^-$ **15**[71] and 1.638(4) Å for the central fc unit of $\mathbf{7_3}$.[48] The shortest iron-iodine distance, *d*(Fe-I), in $[\mathbf{7_3}]^{2+}[I_3]^-$ was found for the terminal iron atoms (*d*(Fe-I) = 4.634(2) and 4.513(2)Å for Fe(1) and Fe(3) versus 5.530(2) Å for *d*(Fe-I) of Fe(2)) showing a closer interaction of the terminal ferrocenium groups with the triiodide counterions. Figure 12 shows the interesting layered structure of $[\mathbf{7_3}]^{2+}[I_3]^-_2 \cdot 2CH_2Cl_2$ in which layers of the linear triiodide counter ions are in between layers of the mixed-valent dicationic tri(ferrocenylsilane).

Table 5. Summary of Crystal Data, Details of Intensity Collection, and Least-Squares Refinement Parameters for $\mathbf{7_5}$ and $[\mathbf{7_3}]^{2+}[I_3]^-_2 \cdot 2CH_2Cl_2$[a]

empirical formula	$C_{58}H_{56}Fe_5Si_4$	$C_{36}H_{42}Cl_4Fe_3I_6Si_2$
M_r	1154.7	1601.6
crystal size, mm	0.30 × 0.35 × 0.10	0.32 × 0.42 × 0.50
crystal class	triclinic	triclinic
space group	$P\bar{1}$	$P\bar{1}$
temp, K	294(2)	173(2)
a, Å	11.764(4)	11.578(3)
b, Å	11.850(2)	13.381(2)
c, Å	12.514(2)	16.245(3)
α, deg	94.85(2)	87.612(12)
β, deg	114.15(2)	75.798(14)
γ, deg	117.66(8)	80.222(12)
V, A^3	1326.1(8)	2404.3(8)
Z	2	2
D_{calc}, g cm^{-3}	1.446	2.212
μ(MoKα), cm^{-1}	14.63	50.54
F(000)	600	1500
ω scan width, deg	0.60	0.46
range *θ* collected, deg	2.0−25.0	2.6−27.0
min., max. trans. coeffs	0.797, 0.876	0.2065, 0.7949
no. reflcns collected	4708	11040
independent reflcns	4353	10511
R_{int}	0.035	0.0906
refined on	*F*	F^2
no. obsd data	3268[$I > 3\sigma(I)$]	5081[$I > 2\sigma(I)$]
R_1	0.0466[$I > 3\sigma(I)$]	0.0726[$I > 2\sigma(I)$]
w*R*, (all data)	0.0745	0.2014
goodness of fit	1.23	0.932
parameters refined	305	470
max density in Δ*F* map, e/A^3	0.66	2.11

[a] *Definition of R indices:* $R_1 = \sum(F_o - F_c)/\sum(F_o)$. $wR = [\sum[w(F_o - F_c)^2]/\sum[w(F_o)^2]]^{1/2}$, $wR_2 = [\sum[w(F_o^2 - F_c^2)^2]/\sum[w(F_o^2)^2]]^{1/2}$.

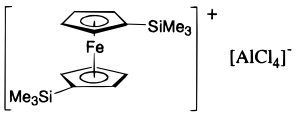

15

Summary

Three series of oligo(ferrocenylsilanes) have been prepared via the ring-opening oligomerization of the strained silicon-bridged [1]ferrocenophane **5**. Studies on these well-defined polynuclear systems have significantly increased our understanding of the solid state and electrochemical properties of ferrocene polymers such as **6**. For example, linear pentamer $\mathbf{7_5}$ has been characterized by single crystal X-ray diffraction and the trans planar zigzag conformation of the central portion of this molecule appears to be an excellent model for the analogous conformation of the high polymer **6** in crystalline domains in the solid state. Because of the negligible inductive effect of the bridging dimethylsilyl groups, conclusions can be drawn based on the through space and through bridge mediated interactions between the iron centers. In silicon-bridged oligo- and poly(ferrocenes), a neutral ferrocene group which is being

(68) $\alpha^2 = \epsilon(4.2 \times 10^{-4})\,\Delta\nu_{1/2}/\nu_{max}d^2$, where d = metal−metal separation (see ref 66).

(69) Powers, M. J.; Meyer, T. J. *J. Am. Chem. Soc.* **1978**, *100*, 4393.

(70) The trication Fc^+-CH_2-fc^+-CH_2-Fc^+ adopts a similar conformation in the solid state; see ref 12.

(71) Foucher, D. A.; Honeyman, C. H.; Lough, A. J.; Manners, I.; Nelson, J. M. *Acta Cryst.* **1995**, *C51*, 1795.

Table 6. Selected Bond Lengths [Å] and Angles [deg] for $\mathbf{7_5}$ and $[\mathbf{7_3}]^{2+}[I_3]^-_2 \cdot 2CH_2Cl_2$

(a) for $\mathbf{7_5}$

Fe(1)−C(1)	2.054 (4)	Fe(2)−C(11)	2.056 (7)	Fe(3)−C(21)	2.053 (6)
Fe(1)−C(2)	2.040 (5)	Fe(2)−C(12)	2.038 (8)	Fe(3)−C(22)	2.034 (6)
Fe(1)−C(3)	2.034 (7)	Fe(2)−C(13)	2.044 (9)	Fe(3)−C(23)	2.012 (17)
Fe(1)−C(4)	2.037 (6)	Fe(2)−C(14)	2.044 (8)	Fe(3)−C(24)	2.019 (21)
Fe(1)−C(5)	2.030 (4)	Fe(2)−C(15)	2.037 (6)	Fe(3)−C(25)	2.025 (9)
Fe(1)−C(6)	2.036 (7)	Fe(2)−C(16)	2.051 (7)	Si(1)−C(1)	1.867 (7)
Fe(1)−C(7)	2.056 (5)	Fe(2)−C(17)	2.038 (9)	Si(1)−C(11)	1.847 (6)
Fe(1)−C(8)	2.044 (5)	Fe(2)−C(18)	2.036 (11)	Si(2)−C(16)	1.856 (6)
Fe(1)−C(9)	2.033 (6)	Fe(2)−C(19)	2.028 (11)	Si(2)−C(21)	1.837 (8)
Fe(1)−C(10)	2.039 (5)	Fe(2)−C(20)	2.028 (7)	Si(1)−C(26)	1.863 (5)
Si(1)−C(27)	1.862 (8)	Si(2)−C(28)	1.831 (8)	Si(2)−C(29)	1.830 (13)
C(1)−Si(1)−C(11)	104.9 (3)				
C(26)−Si(1)−C(27)	109.4 (4)				
C(16)−Si(2)−C(21)	110.2 (3)				
C(28)−Si(2)−C(29)	113.3 (7)				

(b) for $[\mathbf{7_3}]^{2+}[I_3]^-_2 \cdot 2\ CH_2Cl_2$

Fe(1)−C(1)	2.074 (12)	Fe(2)−C(11)	2.026 (11)	Fe(3)−C(21)	2.112 (11)
Fe(1)−C(2)	2.076 (13)	Fe(2)−C(12)	2.010 (14)	Fe(3)−C(22)	2.088 (11)
Fe(1)−C(3)	2.082 (13)	Fe(2)−C(13)	2.027 (14)	Fe(3)−C(23)	2.076 (12)
Fe(1)−C(4)	2.077 (11)	Fe(2)−C(14)	2.016 (14)	Fe(3)−C(24)	2.052 (13)
Fe(1)−C(5)	2.066 (11)	Fe(2)−C(15)	2.035 (13)	Fe(3)−C(25)	2.075 (13)
Fe(1)−C(6)	2.054 (13)	Fe(2)−C(16)	2.038 (12)	Fe(3)−C(26)	2.060 (13)
Fe(1)−C(7)	2.059 (13)	Fe(2)−C(17)	2.013 (13)	Fe(3)−C(27)	2.081 (13)
Fe(1)−C(8)	2.051 (12)	Fe(2)−C(18)	2.020 (20)	Fe(3)−C(28)	2.108 (13)
Fe(1)−C(9)	2.076 (14)	Fe(2)−C(19)	2.038 (13)	Fe(3)−C(29)	2.055 (14)
Fe(1)−C(10)	2.070 (20)	Fe(2)−C(20)	2.032 (13)	Fe(3)−C(30)	2.062 (12)
Si(1)−C(1)	1.859 (13)	Si(2)−C(31)	1.842 (14)	I(1)−I(2)	2.9047 (11)
Si(1)−C(11)	1.851 (12)	Si(2)−C(32)	1.830 (20)	I(3)−I(5)	2.9090 (13)
Si(2)−C(16)	1.815 (13)	Si(2)−C(33)	1.854 (13)	I(4)−I(6)	2.9056 (13)
Si(2)−C(21)	1.863 (13)	Si(2)−C(34)	1.820 (20)	I(7)−I(8)	2.873 (3)
C(1)−Si(1)−C(11)	107.8 (6)				
C(31)−Si(1)−C(32)	114.8 (6)				
C(16)−Si(2)−C(21)	102.6 (5)				
C(33)−Si(2)−C(34)	112.6 (7)				

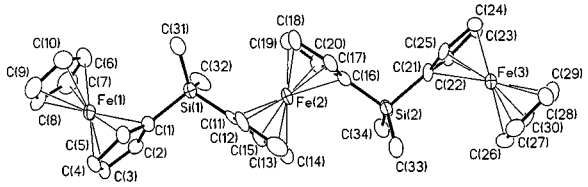

Figure 11. Molecular structure of the mixed-valent dicationic trimer $[\mathbf{7_3}]^{2+}$.

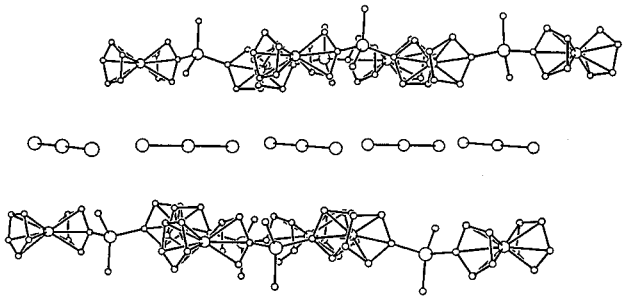

Figure 12. Packing diagram of $[\mathbf{7_3}]^{2+}[I_3]^-_2 \cdot 2CH_2Cl_2$.

oxidized can be neighbored by zero, one or two positively charged ferrocenium groups. As a consequence, up to three redox processes at different $E_{1/2}$ - potentials can be observed in the cyclic voltammograms of the isolated oligo(ferrocenyldimethylsilanes). As the chain length of either "odd" or "even" oligo(ferrocenylsilanes) increases, the electrochemical behavior approaches a situation for which only two reversible redox processes can be observed where the integration ratio in the DPV approaches a 1:1 value which is found for high polymers such as **6**. We found that a ferrocenium group also has a weak long range influence on the oxidation potential of the next nearest ferrocene center resulting in the observation of shoulders or a broadening of the first wave in the cyclic voltammograms. An X-ray diffraction study of $[\mathbf{7_3}]^{2+}$ supports the theory that alternating iron sites of polymers such as **6** are oxidized first, leaving the iron sites in-between to be oxidized at a higher potential. NIR absorption data and IR studies of partially oxidized oligo(ferrocenylsilanes) indicate, that these materials are class II type of mixed-valent compounds with partial electron delocalization.

Experimental Section

Materials. Chlorotrimethylsilane was purchased from Aldrich and distilled under N_2 before use. The silicon-bridged [1]ferrocenophane **5** and $Fe(\eta\text{-}C_5H_4Li)_2 \cdot {}^2/_3TMEDA$ were synthesized as described in literature.[72−74] Aluminum oxide (activated, basic, Brockmann I., standard grade, ~150 Mesh) was purchased from Aldrich and was deactivated with anhydrous ammonia prior to use. Thin layer chromatography (TLC) for analytical purposes and purity control was performed with Sigma-Aldrich silica gel (layer thickness 250 μm, particle size 5−17 μm, pore size 60 Å) on glass plates (20 × 20 cm) using a mixture of 15% dichloromethane in cyclohexane as eluent. The oligomerization reactions were carried out under an atmosphere of prepurified nitrogen using Schlenk techniques. Solvents were dried by standard methods and distilled before use. The oligomers were handled in air.

Equipment. 200, 300, or 400 MHz ^{1}H NMR spectra and 50.3 or 100.5 MHz ^{13}C NMR spectra were recorded on a Varian XL 200, a Varian XL 300 or a Varian Gemini 400 spectrometer. The 79.4 and 59.5 MHz ^{29}Si NMR spectra were recorded on a Varian XL 400 or a Varian XL 300 spectrometer utilizing a DEPT pulse sequence (proton

(72) Rausch, M. D.; Ciappenelli, D. J. *J. Organomet. Chem.* **1967**, *10*, 5025.
(73) Bishop, J. J.; Davison, A.; Katcher, M. L.; Lichtenberg, R. E.; Merrill, J. C.; Smart, J. *J. Organomet. Chem.* **1971**, *27*, 241.
(74) Fischer, A. B.; Kinney, J. B.; Staley, R. H.; Wrighton, M. S. *J. Am. Chem. Soc.* **1979**, *101*, 6501.

decoupled). All solution NMR spectra were referenced externally to TMS. Mass spectra were obtained with the use of a VG 70-250S mass spectrometer operating in an Electron Impact (EI) mode.

Electrochemistry. Both CH_2Cl_2 (reagent grade) and acetonitrile (spectrograde) were stored over and distilled in vacuo from CaH_2. $[NBu_4][PF_6]$ was prepared by metathesis of $[NBu_4]I$ and $[NH_4][PF_6]$, recrystallized from EtOH, and vacuum dried. It was used at a concentration of 0.1 M in all voltammetry experiments. A conventional sample cell operating at ambient temperatures under an atmosphere of nitrogen or argon was used for voltammetry. The experimental reference electrode was a AgCl-coated silver wire. Potentials in this paper are, however, referred to the ferrocene/ferrocenium couple. Ferrocene was added as an internal standard at the end of each experiment. Conversion of the reported potentials to the scale of the aqueous saturated calomel electrode (S.C.E.) requires addition of 0.40 V to the ferrocene/ferrocenium couple. Cyclic voltammetry and chronoamperometry were performed using methods and equipment previously described.[75] A Pt disk electrode with a geometric area of 0.020 cm^2 was employed in CV experiments and one of 0.393 cm^2 was used for chronoamperometry. The electrodes were hand polished on microcloth with diamond pastes of diminishing diameters, finishing with d = 0.25 μm. Differential pulse voltammetry (DPV) was performed with a PARC Model 174A potentiostat, using a small Pt bead working electrode which had been pretreated by a sequence of oxidation by conc. HNO_3 followed by reduction by Fe^{2+}. DPV experiments utilized pulse amplitudes of 25 mV or less and pulse intervals of 2 s. Integration of the areas under DPV curves was accomplished with a Summagraphics board. Digital simulations of DPV curves were performed using a program purchased from Dr. W. Huang (University of New South Wales) and described elsewhere.[76]

Spectroelectrochemistry. Thin-layer spectroelectrochemical cells were used to obtain spectra of oxidation products in both the IR and near-IR regions. In all cases the solvent/electrolyte system was CH_2Cl_2/0.1 M $[NBu_4][PF_6]$. The IR cell and associated procedures have been recently described in detail.[64] The cell path length was 0.06 cm in these experiments. A conventional optically-transparent thin layer electrode (OTTLE) cell with a path length of 0.043 cm and quartz windows was used for vis-near-IR experiments. In both cases the working electrode was constructed from gold mesh (Buckbee-Mears, 100 l pi). Infrared spectra were acquired with a Mattson Polaris FTIR spectrometer operating at 2 cm^{-1} resolution. Optical spectra were measured over the range 330 to 2000 nm using a Cary 14 spectrometer modified by the OLIS Co. (Atlanta, Georgia). The concentration of oligomers in the optical experiments was 12.7 mM.

X-ray Structure Characterization of 7_5 and $[7_3]^{2+}[I_3]^-_2$·2 CH_2Cl_2. Crystals of $[7_3]^{2+}[I_3]^-_2$·2 CH_2Cl_2 were grown from CH_2Cl_2/cyclohexane by a diffusion controlled reaction of a solution of 7_3 with a solution of I_2 in a U-shaped tube. A suitable crystal was mounted in epoxy under a flow of cold nitrogen. Summary of selected crystallographic data are given in Table 5 and selected bond length and angles are given in Table 6. Figures 2 and 11 show the molecules and their labeling schemes. Data for both structures were collected on a Siemens P4 diffractometer using graphite monochromated MoKα radiation (λ = 0.71073 Å). The intensities of three standard reflections measured every 97 reflections, for each crystal, showed less than 4% variation. The data were corrected for Lorentz and polarization effects and for absorption (empirical corrections using Ψ-scans for 7_5 and SHELXA-90[77] for 7_3^{2+}). The structures were solved and refined using the SHELXTL\PC[78] package. Refinement was by full-matrix least-squares. The weighting schemes were $w = 1/\sigma^2(F_o^2) + 0.0020F^2$ for 7_5 and $w = 1/[\sigma^2(F_o^2)+(0.0903P)^2]$ where $P = (F_o^2 + 2F_c^2)/3$ for 7_3^{2+}. Hydrogen atoms were included in calculated positions and treated as riding atoms**.** In 7_3^{2+} the central I atoms of the I_3^- anions lie on crystallographic inversion centers and there are two CH_2Cl_2 solvent molecules of crystallization for each cation molecule.

Synthesis of the Oligomers 7_2−7_9 and 9_2−9_7. To a solution of 1.31 g Fe(η-$C_5H_4Li)_2$·$^2/_3$TMEDA (4.78 mmol) in 50 mL of dry THF at 0 °C, a solution of 1.73 g of the silicon bridged [1]ferrocenophane Fe(η-$C_5H_4)_2SiMe_2$ (**5**) (7.15 mmol) in 10 mL of THF was added at once. After allowing to react for 15 min at 20 °C the reaction mixture was then quenched with 0.2 mL degassed distilled water (11.1 mmol) to obtain 7_2−7_9 or with chlorotrimethylsilane (1.09 g, 10.0 mmol) to afford 9_2−9_7. The reaction mixture was then filtered and the solvent removed under vacuum. The oligomers were separated by column (40 × 3 cm) chromatography using aluminum oxide that was deactivated with anhydrous ammonia and washed with methylene chloride before use and using a gradient of methylene chloride 5−30% in cyclohexane as eluent. Purity of the fractions was checked by TLC and only the fractions of each oligomer showing a single spot were combined. After removal of the solvents, the oligomers were further purified by recrystallization from hexanes.

Synthesis of the Oligomers 8_2−8_7. Ferrocene (1.00 g, 5.38 mmol) was dissolved in 10 mL of THF and was lithiated by dropwise adding *t*-BuLi (2.35 mL of a 1.7 M solution in pentanes, 4.00 mmol) at 0 °C. The reaction mixture was than stirred for 15 min at 0 °C and left to warm to 20 °C. After cooling to 0 °C a solution of the silicon bridged [1]ferrocenophane Fe(η-$C_5H_4)_2SiMe_2$ (**5**) (1.00 g, 4.13 mmol) in 2 mL of THF was added. The reaction was left to warm to 20 °C and stirred for an additional 10 min. Reaction with chlorotrimethylsilane (0.43 g, 4.0 mmol), workup, and isolation as for 7_2−7_9 afforded 8_2−8_7.

Characterization Data for 7_2−7_9, 8_2−8_7, and 9_2−9_7. For 7_2: Amber crystals; mp 97−98 °C; MS (EI, 70 eV) *m/e* 428 (M^+, 100); ^{29}Si NMR (79.5 MHz, $CDCl_3$) δ −6.8 ($SiMe_2$); ^{13}C NMR (50.3 MHz, C_6D_6) δ 73.5, 71.1 (η-C_5H_4), 71.6 (η-C_5H_4, *ipso*C), 68.6 (η-C_5H_5), −0.6 ($SiMe_2$); ^{1}H NMR (400 MHz, $CDCl_3$) δ 0.48 (s, 6H, Me), 4.09 (s, 10H, η-C_5H_5), 4.11 (ps.t, J = 1.6 Hz, 4H, η-C_5H_4), 4.32 (ps.t, J = 1.6 Hz, 4H, η-C_5H_4); TLC R_F = 0.39.

For 7_3: Amber crystals; mp 146 °C; MS (EI, 70 eV) *m/e* 670 (M^+, 100); ^{29}Si NMR (79.5 MHz, $CDCl_3$) δ −6.6 ($SiMe_2$); ^{13}C NMR (50.3 MHz, C_6D_6) δ 73.6, 73.5, 71.7, 71.2 (η-C_5H_4), 71.9, 71.6 (η-C_5H_4, *ipso*C), 68.6 (η-C_5H_5), −0.6 ($SiMe_2$); ^{1}H NMR (400 MHz, $CDCl_3$) δ 0.48 (s, 12H, Me), 4.04 (ps.t, J = 1.6 Hz, 4H, η-C_5H_4), 4.09 (s, 10H, η-C_5H_5), 4.11 (ps.t, J = 1.6 Hz, 4H, η-C_5H_4), 4.23 (ps.t, J = 1.6 Hz, 4H, η-C_5H_4), 4.33 (ps.t, J = 1.6 Hz, 4H, η-C_5H_4); TLC R_F = 0.28.

For 7_4: Amber microcrystals; mp 117−118 °C; MS (EI, 70 eV) *m/e* 912 (M^+, 100); ^{29}Si NMR (79.5 MHz, $CDCl_3$) δ −6.5 ($SiMe_2$, 1Si), −6.6 ($SiMe_2\eta$-C_5H_4, 2Si); ^{13}C NMR (50.3 MHz, C_6D_6) δ 73.6, 73.5, 71.7, 71.2 (η-C_5H_4), 71.9, 71.6 (η-C_5H_4, *ipso*C), 68.6 (η-C_5H_5), −0.5 ($SiMe_2$); ^{1}H NMR (400 MHz, $CDCl_3$) δ 0.45 (s, 6H, Me), 0.47 (s, 12H, Me), 4.01 (ps.t, J = 1.6 Hz, 4H, η-C_5H_4), 4.02 (ps.t, J = 1.6 Hz, 4H, η-C_5H_4), 4.08 (s, 10H, η-C_5H_5), 4.10 (ps.t, J = 1.6 Hz, 4H, η-C_5H_4); 4.21 (ps.t, J = 1.6 Hz, 4H, η-C_5H_4), 4.22 (ps.t, J = 1.6 Hz, 4H, η-C_5H_4), 4.33 (ps.t, J = 1.6 Hz, 4H, η-C_5H_4); TLC R_F = 0.18.

For 7_5: Amber crystals; mp 172 °C; MS (EI, 70 eV) *m/e* 1154 (M^+, 100); ^{29}Si NMR (79.5 MHz, $CDCl_3$) δ −6.5 ($SiMe_2$, 2Si), −6.6 ($SiMe_2$, 2Si); ^{13}C NMR (50.3 MHz, C_6D_6) δ 73.6, 73.5, 71.7, 71.2 (η-C_5H_4), 71.9, 71.8, 71.6 (η-C_5H_4, *ipso*C), 68.6 (η-C_5H_5), −0.6 ($SiMe_2$); ^{1}H NMR (400 MHz, $CDCl_3$) δ 0.45 (s, 12H, Me), 0.47 (s, 12H, Me), 4.01 (m, J = 1.6 Hz, 8H, η-C_5H_4), 4.01 (ps.t, J = 1.6 Hz, 4H, η-C_5H_4), 4.08 (s, 10H, η-C_5H_5), 4.09 (ps.t, J = 1.6 Hz, 4H, η-C_5H_4), 4.20 (m, J = 1.6 Hz, 8H, η-C_5H_4), 4.22 (ps.t, J = 1.6 Hz, 4H, η-C_5H_4), 4.32 (ps.t, J = 1.6 Hz, 4H, η-C_5H_4); TLC R_F = 0.13.

For 7_6: Amber microcrystals; mp 136−137 °C; MS (EI, 70 eV) *m/e* 1397 (M^+, 82); ^{29}Si NMR (79.5 MHz, $CDCl_3$) δ −6.5 ($SiMe_2$, 3Si), −6.7 ($SiMe_2$, 2Si); ^{13}C NMR (50.3 MHz, C_6D_6) δ 73.6, 73.5, 71.7, 71.2 (η-C_5H_4), 71.9, 71.8, 71.6 (η-C_5H_4, *ipso*C), 68.6 (η-C_5H_5), −0.6 ($SiMe_2$); ^{1}H NMR (400 MHz, $CDCl_3$) δ 0.44 (s, 18H, Me), 0.46 (s, 12H, Me), 4.00 (ps.t, J = 1.6 Hz, 12H, η-C_5H_4), 4.01 (ps.t, J = 1.6 Hz, 4H, η-C_5H_4), 4.07 (s, 10H, η-C_5H_5), 4.09 (ps.t, J = 1.6 Hz, 4H, η-C_5H_4), 4.19 (ps.t, J = 1.6 Hz, 12H, η-C_5H_4), 4.21 (ps.t, J = 1.6 Hz, 4H, η-C_5H_4), 4.32 (ps.t, J = 1.6 Hz, 4H, η-C_5H_4); TLC R_F = 0.09.

For 7_7: Amber microcrystals; mp 146−147 °C; MS (EI, 70 eV) *m/e* 1639 (M^+, 16); ^{29}Si NMR (79.5 MHz, $CDCl_3$) δ −6.5 ($SiMe_2$, 4Si), −6.7 ($SiMe_2$, 2Si); ^{13}C NMR (50.3 MHz, C_6D_6) δ 73.6, 73.5, 71.7, 71.2 (η-C_5H_4), 71.9, 71.8, 71.6 (η-C_5H_4, *ipso*C), 68.6 (η-C_5H_5), −0.6 ($SiMe_2$); ^{1}H NMR (400 MHz, $CDCl_3$) δ 0.44 (s, 24H, Me), 0.46 (s, 12H, Me), 4.00 (ps.t, J = 1.6 Hz, 16H, η-C_5H_4), 4.01 (ps.t, J = 1.6 Hz, 4H, η-C_5H_4), 4.07 (s, 10H, η-C_5H_5), 4.09 (ps.t, J = 1.6 Hz, 4H,

(75) Chin, T. T.; Geiger, W. E.; Rheingold, A. L. *J. Am. Chem. Soc.* **1996**, *118*, 5002.

(76) Huang, W.; Henderson, T.; Bond, A. M.; Oldham, K. B. *Anal. Chim. Acta* **1995**, *304*, 1.

(77) Sheldrick, G. M. SHELXA-90, Program for Absorption Correction; University of Göttingen, Germany.

(78) Sheldrick, G. M. SHELXTL\PC V5.0, Siemens Analytical X-ray; Instruments Inc., Madison, WI, U. S. A.

η-C_5H_4), 4.20 (ps.t, J = 1.6 Hz, 16H, η-C_5H_4), 4.21 (ps.t, J = 1.6 Hz, 4 H, η-C_5H_4), 4.32 (ps.t, J = 1.6 Hz, 4H, η-C_5H_4); TLC R_F = 0.07.

For **7$_8$**: Amber powder; mp 140−142 °C; MS (EI, 70 eV) *m*/*e* 1881 (M^+, 3); ^{29}Si NMR (79.5 MHz, $CDCl_3$) δ −6.5 ($SiMe_2$, 5Si), −6.7 ($SiMe_2$, 2Si); ^{13}C NMR (50.3 MHz, C_6D_6) δ 73.6, 73.5, 71.7, 71.2 (η-C_5H_4), 71.9, 71.8, 71.6 (η-C_5H_4, *ipso*C), 68.6 (η-C_5H_5), −0.6 ($SiMe_2$); ^{1}H NMR (400 MHz, $CDCl_3$) δ 0.44 (s, 30H, Me), 0.46 (s, 12H, Me), 3.99 (ps.t, J = 1.6 Hz, 20H, η-C_5H_4), 4.01 (ps.t, J = 1.6 Hz, 4H, η-C_5H_4), 4.08 (s, 10H, η-C_5H_5), 4.08 (ps.t, J = 1.6 Hz, 4H, η-C_5H_4), 4.20 (ps.t, J = 1.6 Hz, 20H, η-C_5H_4), 4.21 (ps.t, J = 1.6 Hz, 4H, η-C_5H_4), 4.32 (ps.t, J = 1.6 Hz, 4H, η-C_5H_4); TLC R_F = 0.04.

For **7$_9$**: Amber powder; mp 152−153 °C; MS (EI, 70 eV) *m*/*e* 2124 (M^+, 1); ^{29}Si NMR (79.5 MHz, $CDCl_3$) δ −6.5 ($SiMe_2$, 6Si), −6.7 ($SiMe_2$, 2Si); ^{13}C NMR (50.3 MHz, C_6D_6) δ 73.6, 73.5, 71.7, 71.2 (η-C_5H_4), 71.9, 71.8, 71.6 (η-C_5H_4, *ipso*C), 68.6 (η-C_5H_5), −0.6 ($SiMe_2$); ^{1}H NMR (400 MHz, $CDCl_3$) δ 0.44 (s, 36H, Me), 0.46 (s, 12H, Me), 3.99 (ps.t, J = 1.6 Hz, 24H, η-C_5H_4), 4.01 (ps.t, J = 1.6 Hz, 4H, η-C_5H_4), 4.07 (s, 10H, η-C_5H_5), 4.09 (ps.t, J = 1.6 Hz, 4H, η-C_5H_4), 4.20 (ps.t, J = 1.6 Hz, 24H, η-C_5H_4), 4.21 (ps.t, J = 1.6 Hz, 4H, η-C_5H_4), 4.32 (ps.t, J = 1.6 Hz, 4H, η-C_5H_4); TLC R_F = 0.03.

For **8$_2$**: Amber oil; MS (EI, 70 eV) *m*/*e* 500 (M^+, 100); ^{29}Si NMR (79.5 MHz, $CDCl_3$) δ −3.1 ($SiMe_3$), −6.6 ($SiMe_2$); ^{13}C NMR (50.3 MHz, $CDCl_3$) δ 73.1, 73.0, 71.4, 71.3, 71.1, 70.7 (η-C_5H_4), 72.8 ppm (η-C_5H_4, *ipso*C-$SiMe_3$), 68.8 (η-C_5H_5), −0.1 ($SiMe_3$), −0.9 ($SiMe_2$); ^{1}H NMR (400 MHz, $CDCl_3$) δ 0.21 (s, 9H, $SiMe_3$), 0.49 (s, 6H, $SiMe_2$), 4.02 (ps.t, J = 1.6 Hz, 2H, η-C_5H_4), 4.07 (ps.t, J = 1.6 Hz, 2H, η-C_5H_4), 4.09 (s, 5H, η-C_5H_5), 4.11 (ps.t, J = 1.6 Hz, 2H, η-C_5H_4), 4.23 (ps.t, J = 1.6 Hz, 2H, η-C_5H_4), 4.28 (ps.t, J = 1.6 Hz, 2H, η-C_5H_4), 4.33 (ps.t, J = 1.6 Hz, 2H, η-C_5H_4); Anal. C 59.33 (calcd. 60.00), H 6.51 (calcd. 6.40); TLC R_F = 0.46.

For **8$_3$**: Amber oil; MS (EI, 70 eV) *m*/*e* 742 (M^+, 100); ^{29}Si NMR (79.5 MHz, $CDCl_3$) δ −3.1 ($SiMe_3$), −6.5, −6.6 ($SiMe_2$); ^{13}C NMR (50.3 MHz, $CDCl_3$) δ 73.1, 73.0, 71.3, 71.2, 70.7 (η-C_5H_4), 72.8 (η-C_5H_4, *ipso*C-$SiMe_3$), 68.2 (η-C_5H_5), −0.2 ($SiMe_3$), −0.9 ($SiMe_2$); ^{1}H NMR (400 MHz, $CDCl_3$) δ 0.21 (s, 9H, $SiMe_3$), 0.48 (s, s, 12H, $SiMe_2$), 4.01 (m, 6H, η-C_5H_4), 4.06 (ps.t, J = 1.6 Hz, 2H, η-C_5H_4), 4.08 (s, 5H, η-C_5H_5), 4.10 (ps.t, J = 1.6 Hz, 2H, η-C_5H_4), 4.22 (m, J = 1.6 Hz, 6H, η-C_5H_4), 4.28 (ps.t, J = 1.6 Hz, 2H, η-C_5H_4), 4.33 (ps.t, J = 1.6 Hz, 2H, η-C_5H_4); TLC R_F = 0.36.

For **8$_4$**: Amber powder; mp 90 °C; MS (EI, 70 eV) *m*/*e* 984 (M^+, 100); ^{29}Si NMR (79.5 MHz, $CDCl_3$): δ −3.1 ($SiMe_3$), δ −6.5, −6.6 ($SiMe_2$); ^{13}C NMR (50.3 MHz, $CDCl_3$) δ 73.1, 73.0, 71.4, 71.2, 71.1, 70.7 (η-C_5H_4), 72.8 (η-C_5H_4, *ipso*C-$SiMe_3$), 68.2 (η-C_5H_5), −0.1 ($SiMe_3$), −0.9 ($SiMe_2$);^{1}H NMR (400 MHz, $CDCl_3$) δ 0.21 (s, 9 H, $SiMe_3$), 0.45 (s, 6H, $SiMe_2$), 0.48 (s, s, 12H, $SiMe_2$), 4.01 (m, 10H, η-C_5H_4), 4.06 (ps.t, J = 1.6 Hz, 2H, η-C_5H_4), 4.08 (s, 5H, η-C_5H_5), 4.10 (ps.t, J = 1.6 Hz, 2 H, η-C_5H_4), 4.21 (m, 10H, η-C_5H_4), 4.28 (ps.t, J = 1.6 Hz, 2H, η-C_5H_4), 4.33 (ps.t, J = 1.6 Hz, 2H, η-C_5H_4); TLC R_F = 0.27.

For **8$_5$**: Amber powder; mp 115 °C; MS (EI, 70 eV) *m*/*e* 1227 (M^+, 100); ^{29}Si NMR (79.5 MHz, $CDCl_3$) δ −3.1 ($SiMe_3$), δ −6.5, −6.6 ($SiMe_2$); ^{13}C NMR (50.3 MHz, $CDCl_3$) δ 73.2, 71.5, 71.2, 70.7 (η-C_5H_4), 72.9 (η-C_5H_4, *ipso*C-$SiMe_3$), 68.2 (η-C_5H_5), −0.2 ($SiMe_3$), −0.9 ($SiMe_2$); ^{1}H NMR (400 MHz, $CDCl_3$) δ 0.21 (s, 9H, $SiMe_3$), 0.45 (s, 12H, $SiMe_2$), 0.48 (s, s, 12H, $SiMe_2$), 4.01 (m, 14H, η-C_5H_4), 4.06 (ps.t, J = 1.6 Hz, 2H, η-C_5H_4), 4.09 (s, 5H, η-C_5H_5), 4.10 (ps.t, J = 1.6 Hz, 2H, η-C_5H_4), 4.22 (m, 14H, η-C_5H_4), 4.28 (ps.t, J = 1.6 Hz, 2H, η-C_5H_4), 4.33 (ps.t, J = 1.6 Hz, 2H, η-C_5H_4); Anal. C 59.81 (calcd. 59.66), H 6.21 (calcd. 6.03); TLC R_F = 0.21.

For **8$_6$**: Amber powder; mp 115 °C; MS (EI, 70 eV) *m*/*e* 1471 (M^+, 57); ^{29}Si NMR (79.5 MHz, $CDCl_3$) δ −3.1 ($SiMe_3$), −6.5, −6.7 ($SiMe_2$); ^{13}C NMR (50.3 MHz, $CDCl_3$) δ 73.2, 73 1, 71.5, 71.2, 70.7 (η-C_5H_4), 72.9 (η-C_5H_4, *ipso*C-$SiMe_3$), 68.2 (η-C_5H_5), −0.9 ($SiMe_2$); ^{1}H NMR (400 MHz, $CDCl_3$) δ 0.21 (s, 9H, $SiMe_3$), 0.45 (s, 18H, $SiMe_2$), 0.48 (s, s, 12H, $SiMe_2$), 4.01 (m, 18H, η-C_5H_4), 4.06 (ps.t, J = 1.6 Hz, 2H, η-C_5H_4), 4.09 (s, 5H, η-C_5H_5), 4.10 (ps.t, J = 1.6 Hz, 2H, η-C_5H_4), 4.22 (m, 18H, η-C_5H_4), 4.28 (ps.t, J = 1.6 Hz, 2H, η-C_5H_4), 4.33 (ps.t, J = 1.6 Hz, 2H, η-C_5H_4). TLC R_F = 0.15.

For **8$_7$**: Amber powder; mp 102 °C; MS (EI, 70 eV) *m*/*e* 1710 (M^+, 7); ^{29}Si NMR (79.5 MHz, $CDCl_3$) δ −3.1 ($SiMe_3$), −6.5, −6.7 ($SiMe_2$); ^{13}C NMR (50.3 MHz, $CDCl_3$) δ 73.2, 71.5, 71.3, 70.7 (η-C_5H_4), 68.2 (η-C_5H_5), −0.9 ($SiMe_2$); ^{1}H NMR (400 MHz, $CDCl_3$) δ 0.21 (s, 9H, $SiMe_3$), 0.45 (s, 24H, $SiMe_2$), 0.48 (s, s, 12H, $SiMe_2$), 4.02 (m, 22H, η-C_5H_4), 4.06 (ps.t, J = 1.6 Hz, 2H, η-C_5H_4), 4.09 (s, 5H, η-C_5H_5), 4.10 (ps.t, J = 1.6 Hz, 2H, η-C_5H_4), 4.21 (m, 22H, η-C_5H_4), 4.28 (ps.t, J = 1.6 Hz, 2H, η-C_5H_4), 4.33 (ps.t, J = 1.6 Hz, 2H, η-C_5H_4); TLC R_F = 0.10.

For **9$_2$**: Amber oil; MS (EI, 70 eV) *m*/*e* 572 (M^+, 100); ^{29}Si NMR (59.6 MHz, C_6D_6) δ −3.3 ($SiMe_3$), −6.4 ($SiMe_2$); ^{13}C NMR (50.3 MHz, C_6D_6) δ 73.4, 73.3, 71.7, 71.5 (η-C_5H_4), 72.1, 68.2 (η-C_5H_4, *ipso*C), 0.0 ($SiMe_3$), −0.6 ($SiMe_2$); ^{1}H NMR (200 MHz, C_6D_6) δ 0.23 (s, 18 H, $SiMe_3$), 0.52 (s, 6 H, $SiMe_2$), 4.00, 4.08, 4.22, 4.23 (ps.t, J = 1.6 Hz, 16 H, η-C_5H_4); Anal. C 58.60 (calcd.: 58.74), H 7.10 (calcd.: 7.04); TLC R_F = 0.42.

For **9$_3$**: Amber solid; mp 67−68 °C; MS (EI, 70 eV) *m*/*e* 814 (M^+, 100); ^{29}Si NMR (59.6 MHz, C_6D_6) δ −3.3 ($SiMe_3$), δ −6.4 ($SiMe_2$); ^{13}C NMR (50.3 MHz, C_6D_6) δ 73.6, 73.4, 73.3, 71.7, 71.5 (η-C_5H_4), 72.2, 68.6 (η-C_5H_4, *ipso*C), 0.0 ($SiMe_3$), −0.6 ($SiMe_2$); ^{1}H NMR (200 MHz, C_6D_6) δ 0.23 (s, 18 H, $SiMe_3$), 0.52 (s, 12 H, $SiMe_2$), 4.00, 4.08, 4.22, 4.23 (ps.t, J = 1.6 Hz, 24 H, η-C_5H_4); TLC R_F = 0.31.

For **9$_4$**: Amber solid; mp 87−89 °C; MS (EI, 70 eV) *m*/*e* 1056 (M^+, 100); ^{29}Si NMR (59.6 MHz, C_6D_6) δ −3.3 ($SiMe_3$), δ −6.4 ($SiMe_2$); ^{13}C NMR (50.3 MHz, C_6D_6) δ 73.6, 73.4, 73.3, 71.7, 71.5 (η-C_5H_4), 72.2, 68.6 (η-C_5H_4, *ipso*C), 0.0 ($SiMe_3$), −0.6 ($SiMe_2$); ^{1}H NMR (200 MHz, C_6D_6) δ 0.23 (s, 18 H, $SiMe_3$), 0.52, (s, 18 H, $SiMe_2$), 4.00, 4.08, 4.22, 4.23 (ps.t, J = 1.6 Hz, 32 H, η-C_5H_4); Anal. C 58.41 (calcd. 59.09), H 6.36 (calcd. 6.48); TLC R_F = 0.23.

For **9$_5$**: Amber microcrystals; mp 118°C; MS (EI, 70 eV) *m*/*e* 1298 (M^+, 100); ^{29}Si NMR (59.6 MHz, C_6D_6) δ −3.3 ($SiMe_3$), δ −6.4 ($SiMe_2$); ^{13}C NMR (50.3 MHz, C_6D_6) δ 73.6, 73.4, 73.3, 71.7, 71.5 (η-C_5H_4), 72.2, 68.6 (η-C_5H_4, *ipso*C), 0.0 ($SiMe_3$), −0.6 ($SiMe_2$); ^{1}H NMR (200 MHz, C_6D_6) δ 0.23 (s, 18 H, $SiMe_3$), 0.52 (s, 24 H, $SiMe_2$), 4.00, 4.08, 4.22, 4.23 (ps.t, J = 1.6 Hz, 40 H, η-C_5H_4); TLC R_F = 0.17.

For **9$_6$**: Amber powder; mp 124−126°C; MS (EI, 70 eV) *m*/*e* 1540 (M^+, 100); ^{29}Si NMR (59.6 MHz, C_6D_6) δ −3.3 ($SiMe_3$), −6.4 ($SiMe_2$); ^{13}C NMR (50.3 MHz, C_6D_6) δ 73.6, 73.4, 73.3, 71.7, 71.5 (η-C_5H_4), 72.2, 68.6 (η-C_5H_4, *ipso*C), 0.0 ($SiMe_3$), −0.6 ($SiMe_2$); ^{1}H NMR (200 MHz, C_6D_6) δ 0.23 (s, 18 H, $SiMe_3$), 0.52 (s, 30 H, $SiMe_2$), 4.00, 4.08, 4.22, 4.23 (ps.t, J = 1.6 Hz, 48 H, η-C_5H_4); Anal. C 59.21 (calcd. 59.23), H 6.24 (calcd. 6.28); TLC R_F = 0.12.

For **9$_7$**: Amber powder; mp 131 °C; MS (EI, 70 eV) *m*/*e* 1782 (M^+, 52); ^{29}Si NMR (59.6 MHz, C_6D_6) δ −3.3 ($SiMe_3$), −6.4 ($SiMe_2$); ^{13}C NMR (50.3 MHz, C_6D_6) δ 73.6, 73.4, 73.3, 71.7, 71.5 (η-C_5H_4), 72.2, 68.6 (η-C_5H_4, *ipso*C), 0.0 ($SiMe_3$), −0.6 ($SiMe_2$); ^{1}H NMR (200 MHz, C_6D_6) δ 0.23 (s, 18 H, $SiMe_3$), 0.52 (s, 36 H, $SiMe_2$), 4.00, 4.08, 4.22, 4.23 (ps.t, J = 1.6 Hz, 56 H, η-C_5H_4); TLC R_F = 0.07.

Acknowledgment. R.R. and I.M. thank the Natural Science and Engineering Research Council of Canada (NSERC) for financial support. I.M. also thanks the Alfred P. Sloan Foundation for a Research Fellowship (1994−1998). R.R. thanks the University of Toronto for a Connaught Scholarship (1994−1995) and the Government of Ontario for an Ontario Graduate Scholarship (1995−1996). Research at the University of Vermont was supported by the National Science Foundation (CHE 91-16332). We also thank Randall Perry for obtaining single crystals of [**7$_3$**]$^{2+}$[I_3]$^-_2$ and Ms. Tong Jiang for the generation of Figure 3.

Supporting Information Available: Tables of atomic coordinates, bond angles and bond length, equivalent isotropic displacement parameters, anisotropic thermal parameters and H-atom coordinates and isotropic displacement coefficients for **7$_5$** and [**7$_3$**]$^{2+}$[I_3]$^-_2$·2 CH_2Cl_2 (16 pages). See any current masthead page for ordering and Internet access instructions.

JA962470S